





Review

A Review of Artificial Intelligence Methods in Predicting Thermophysical Properties of Nanofluids for Heat Transfer Applications

Ankan Basu ¹, Aritra Saha ², Sumanta Banerjee ³, Prokash C. Roy ⁴ and Balaram Kundu ^{4,*}¹ Department of Computer Science and Engineering, Jadavpur University, Kolkata 700032, India² Department of Computer Science and Engineering, Heritage Institute of Technology, Kolkata 700107, India³ Department of Mechanical Engineering, Heritage Institute of Technology, Kolkata 700107, India⁴ Department of Mechanical Engineering, Jadavpur University, Kolkata 700032, India

* Correspondence: bkundu@mech.net.in

Abstract: This present review explores the application of artificial intelligence (AI) methods in analysing the prediction of thermophysical properties of nanofluids. Nanofluids, colloidal solutions comprising nanoparticles dispersed in various base fluids, have received significant attention for their enhanced thermal properties and broad application in industries ranging from electronics cooling to renewable energy systems. In particular, nanofluids' complexity and non-linear behaviour necessitate advanced predictive models in heat transfer applications. The AI techniques, which include genetic algorithms (GAs) and machine learning (ML) methods, have emerged as powerful tools to address these challenges and offer novel alternatives to traditional mathematical and physical models. Artificial Neural Networks (ANNs) and other AI algorithms are highlighted for their capacity to process large datasets and identify intricate patterns, thereby proving effective in predicting nanofluid thermophysical properties (e.g., thermal conductivity and specific heat capacity). This review paper presents a comprehensive overview of various published studies devoted to the thermal behaviour of nanofluids, where AI methods (like ANNs, support vector regression (SVR), and genetic algorithms) are employed to enhance the accuracy of predictions of their thermophysical properties. The reviewed works conclusively demonstrate the superiority of AI models over the classical approaches, emphasizing the role of AI in advancing research for nanofluids used in heat transfer applications.

Keywords: nanofluid; machine learning; heat transfer augmentation; viscosity; thermal conductivity; specific heat capacity



Citation: Basu, A.; Saha, A.; Banerjee, S.; Roy, P.C.; Kundu, B. A Review of Artificial Intelligence Methods in Predicting Thermophysical Properties of Nanofluids for Heat Transfer Applications. *Energies* **2024**, *17*, 1351. <https://doi.org/10.3390/en17061351>

Academic Editor: Artur Blaszczuk

Received: 31 December 2023

Revised: 28 February 2024

Accepted: 5 March 2024

Published: 12 March 2024



Copyright: © 2024 by the authors. Licensee MDPI, Basel, Switzerland. This article is an open access article distributed under the terms and conditions of the Creative Commons Attribution (CC BY) license (<https://creativecommons.org/licenses/by/4.0/>).

1. Introduction

Nanofluids are colloidal solutions of nanometre-sized particles in certain base fluids. The nanoparticles can be obtained from various solids such as Cu, CuO, Al₂O₃, and carbon nanotubes (CNT). Base fluids may include water, EG, MO, and others. Nanometre-sized particles are crucial as they are more stable in the colloidal system than microparticles due to vigorous Brownian motion [1]. In addition, the nanoparticles do not clog conduits in equipment, which renders nanofluids attractive in engineering and technological applications.

Numerous techniques, including direct evaporation [2,3], laser ablation [4,5], submerged arc nanoparticle synthesis systems [6,7], and others, can be used to prepare nanofluids. These techniques can be categorized as One-step and Two-step methods. The synthesis of nanoparticles and their dispersion in the base fluid co-occurs in the One-step Method; in the Two-step Method, nanoparticles and their mixing in base fluids occur in different steps. However, nanoparticles' high surface activity and enhanced surface-area-volume ratio make them prone to aggregation; the nanoparticles must be stabilized to avoid aggre-

gation [8]. Various techniques can achieve this stabilization, such as surface treatment [9] or using surfactants or polymers [10], as well as other methods.

Adding nanoparticles in base fluids alters the base fluids' rheological and thermo-physical properties, often rendering exciting and novel engineering applications. Many kinds of nanofluids have been synthesized for various applications, which include brake fluids [11], coolant fluids [12], home refrigerators [13], magnetic-field-assisted hyperthermia [14], delivery of drugs [15], optical filters [16], defect sensors [17], cosmetics, and solar devices [18,19]. As the synthesis techniques do away with sedimentation, clogging, and fouling, the application of nanofluids as efficient coolants has attracted significant attention from researchers over the decades [20–23]. In addition, better optical and radiative properties and higher thermal conductivity and heat capacity values make nanofluids better than conventional working fluids in thermal engineering applications.

In particular, the enhanced heat transfer rates, higher values of critical heat flux, and enhanced thermal conductivity of nanofluids are three primal characteristics that make them promising coolants. For instance, machines must efficiently dissipate significant heat during their operation. The equipment's electrical and mechanical components could heat up beyond desirable levels if the generated heat does not adequately disperse. This fact lowers the system's overall energy efficiency or potentially degrades the performance of mechanical and electrical components [24]. In these situations, the use of efficient coolants becomes necessary.

A notable trend in the research and development on nanofluids has been the significant rise in sustainable and renewable energy systems [25]. Many renewable energy sources, including solar, wind, and geothermal energy, have found extensive applications for nanofluids.

For example, an Al_2O_3 –water nanofluid as a coolant in wind turbines has been proposed by De Risi et al. [26]. This nanofluid significantly lowers the maximum temperature generated in the machinery. Rostamzadeh and Rostami [27] have used a nanofluid as the working fluid to transfer heat produced in wind turbine generators (employed to desalinate seawater). The CuO /water nanofluid has shown the highest cooling efficiency in the desalination process among the five nanofluids, as tested by the authors. In geothermal borehole heat exchangers, nanofluids can produce promising heat transfer enhancement [28–30].

A literature review has shown that nanofluids have been the preferred working fluid in solar collectors over the last two decades [31–33]. Solar collectors absorb solar radiation and convert it into usable thermal energy stored or transported by the working fluid [34–36]. Adequate energy flow between the working fluid and the absorber is necessary. Sardarabadi et al. [37] have found that a SiO_2 –water nanofluid, respectively at 1% weight and 3% weight concentrations, could enhance the collector efficiency by 7.6% and 12.8%, as compared with the pure water in the PV/T system.

The thermophysical properties of working fluids, such as viscosity, SHC (Specific Heat Capacity), and TC (Thermal Conductivity), are significant factors that impact engineering and industrial uses. Several variables, including the type and/or size of the nanoparticles and the characteristics of the base fluids, affect these properties. For instance, for a given particle size (say 50 nm), 'N' types of nanoparticles and 'M' types of base fluids can theoretically yield ($N \times M$) types of nanofluids. Multiple high-thermal-conductivity nanoparticles, which include graphene [38], SiO_2 [39], MgO [40], SiC [41], Ni [42], TiO_2 [43], Cu [44], CuO [45], Fe_3O_4 [46], CNTs [47], Ag [48], Al_2O_3 [48,49], CeO_2 [50], and others, have been experimented with for preparing nanofluids.

Heat exchangers are an essential tool in engineering applications. With the adoption of heat exchangers, high-efficiency heat transfer enhancement is always possible. Using a fluid with superior thermal properties is the most promising technique to improve heat transfer rates and effectiveness in heat exchangers [51]. Nanofluids have been used in various heat exchangers in recent years. According to recent studies conducted in shell-and-tube heat exchangers, nanofluids with nanoparticles, such as Ag [52], TiO_2 [53], CuO [54], Al_2O_3 [53,55], and graphene oxide [56], have shown better thermal performances

as compared with their respective base fluids. A range of nanofluids, such as Al_2O_3 -water [57], Ag-EG/water [58,59], fly ash with metal-oxides-water [60], Cu/CuO/CNT-water [61], Fe_3O_4 -water [62,63], and MgO-oil [64], have all been investigated for double-pipe heat exchangers. This shows that a variety of nanoparticles can effectively improve the heat transfer performance of plate heat exchangers, which include Al_2O_3 [65–67], CuO [68], TiO_2 [69], Ag [70–72], SiO [73,74], CNT [75,76], and ZnO [77].

Nanofluids exhibit complex thermophysical properties, and their relationships with heat transfer, radiative and optical performance, and fluid flow are non-linear. The performance of heat transfer processes and/or devices depends on the properties of working fluids. The accurate measurements and prediction of nanofluid thermophysical properties are essential. However, a variety of factors affect a nanofluid's thermophysical properties, such as concentration, kind, size, and shape of the nanoparticles, the temperature of the system in which they are suspended, the shear rates, the pH level, the preparation process, the kind of base fluid [78], the flow conditions, etc. As a result, determining the thermophysical properties of nanofluids is a challenging and ongoing endeavour in thermo-fluids research. Measurements of these properties through experimentation are expensive and usually yield a small (parametric) dataset. However, for numerical and/or analytical approaches, the knowledge of property values and interactions between the base fluids and the nanoparticles becomes necessary under various operational parameters (for validation purposes).

These complex mathematical and physical models can be avoided largely by using AI techniques like GA and ML [79]. These are also more efficient and cost-saving than experimental procedures. Consequently, AI techniques like ML and GA hold significant potential and warrant greater utilization in the nanofluid and renewable energy sectors. These techniques present new strategies, promising a bright future in nanofluid research. The use of AI techniques in nanofluid research has steadily grown in the past decade. This trend is depicted in Figure 1, which indicates the number of papers on AI applications in the nanofluid domain per year, as retrieved from the Scopus database.

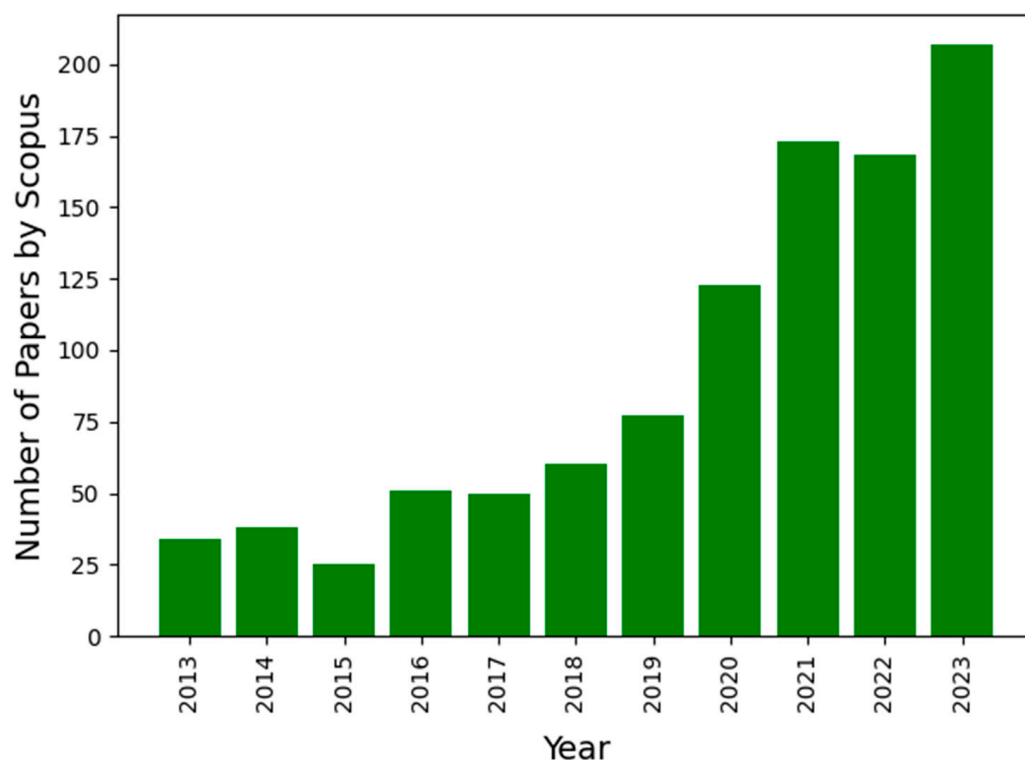


Figure 1. Bar chart representing the number of AI-related nanofluid papers per year as retrieved from Scopus database.

In recent years, several researchers have used AI, ML, and GA techniques to model nanofluids' thermophysical properties. The present work comprehensively reviews the recent works on nanofluids' thermophysical property modelling using AI techniques. From the surveyed literature, it has been observed that AI models outperform traditional methods, showcasing their potential for widespread application. This is due to the capability of AI methods to model the complex behaviour of nanofluids, which is difficult to capture by traditional theoretical models. However, specific challenges deserve mention. These primarily include enhancing the generalizability and addressing data availability, among other issues. The field, though nascent and upcoming, is growing steadily and has the potential to contribute as a novel alternative and an economically viable method for predicting nanofluid thermophysical properties for academic and industrial purposes.

This review paper begins with a brief description of the essential thermophysical properties of nanofluids, followed by a concise overview of the most common AI techniques and algorithms used in the relevant literature surveyed. A survey of recent published works is then carried out, coupled with an analysis of the investigations, the methodologies adopted, and the principal outcomes from these studies. The paper concludes with research gaps and potential avenues for possible future work.

2. Thermophysical Properties of Nanofluids

A brief explanation and overview of the main thermophysical properties of nanofluids, viz. TC, viscosity, and SHC, along with different correlation-based models for the same, are presented in the following subsections.

2.1. Thermal Conductivity

The TC is the ability of a substance to transfer heat by the phenomenon of conduction. Here, thermal energy is transferred by the kinetic energy of the molecules, atoms, ions, or constituent particles in motion. Unlike convection, no macroscopic movement of bulk substance occurs in conduction.

One of the main drawbacks in many industrial applications is the typically low values of TC of heat transfer fluids. Intending to increase the (effective) heat conductivity of the working medium, dispersing solid particles in liquids has garnered interest for almost a century. This technique is motivated by numerous possible uses for efficient TC augmentation, which include electronics cooling systems, the automobile industry, and the biomedical field, to mention a few.

The published literature presents several methods for measuring the TC, including the steady-state parallel plate method, the three-omega approach, the transient hot-wire method, and the thermal constants analyser methods. The TC enhancement of a nanofluid is affected by the fluid temperature, the solid nanoparticles' TC, their volume fraction, and their size. In general, adding nanoparticles to a base fluid increases its heat conductivity. A prevalent finding is that, at higher temperature values, the increase in TC is more pronounced for higher particle fractions [80–83], which renders particle-dispersed liquid systems effective as heat-removal agents in applications with higher thermal loads. Relative TC, a measure of enhancement (of heat transfer rates) relative to the base fluid, is the ratio of the TCs of the nanofluid to that of the base fluid. It was reported that the relative TC increases when concentration increases. It turns out that the temperature, agglomeration, shape, size, and surface functionalization of the nanoparticles, as well as their Brownian motion within the base fluid, all affect the TC of the nanofluids.

Numerous researchers have worked to create numerical models for predicting a nanofluid's TC. Some of them [84–87] are summarised in Table 1.

Table 1. A few correlations-based models for nanofluid thermal conductivity.

Authors	Formula
Maxwell, 1881 [84]	$k_{nf} = \frac{k_{np} + 2k_{bf} + 2(k_{np} - k_{bf})\varphi}{k_{np} + 2k_{bf} - (k_{np} - k_{bf})\varphi} k_{bf}$
Hamilton and Crosser, 1962 [85]	$k_{nf} = \frac{k_{np} + (n-1)k_{bf} - (n-1)(k_{np} - k_{bf})\varphi}{k_{np} + (n-1)k_{bf} + (k_{bf} - k_{np})\varphi} k_{bf}$
Koo and Kleinstreuer, 2004 [86]	$k_{nf} = \frac{k_{np} + 2k_{bf} - 2(k_{bf} - k_{np})\varphi}{k_{np} + 2k_{bf} + (k_{bf} - k_{np})\varphi} k_{bf} + 5 \times 10^4 \beta \varphi \rho_{bf} C_{p,bf} \sqrt{\frac{\kappa T}{\rho_{np} d_{np}}} f(T, \varphi)$ $f(T, \varphi) = (-6.04\varphi + 0.4705)T + (1722.3\varphi - 134.63)$
Sundar et al., 2021 [87]	$k_{hnf} = 1.041k_{bf} \left[(1 + \varphi)^{0.39} \times \left(\frac{T_{min}}{T_{max}} \right)^{0.383 \times 10^{-1}} \right]$

In the equations presented in Table 1, the symbol k_{nf} refers to the TC of the nanofluid, k_{np} indicates the TC of the nanoparticle, k_{bf} is the TC of the base fluid, and k_{hnf} is the TC of the hybrid nanofluid. The symbol φ represents the volume fraction, ρ_{bf} is the density of the base fluid, ρ_{np} is the density of the nanoparticle, d_{np} is the diameter of the nanoparticle, $C_{p,bf}$ is the SHC of the base fluid, κ is the Boltzmann constant, T is the temperature of the nanofluid, and β is a function that depends on the volume fraction [86]. The equation presented by the Hamilton and Crosser model, for instance, uses the shape factor to determine the effective TC of a fluid containing spherical- and cylindrical-shaped nanoparticles. The factor n depends on the particle shape and the shape factor [85].

To date, no standard general model forecasts the TC of either unitary or hybrid nanofluids. In recent years, several research approaches have been conducted for AI methods to predict nanofluids' TC [88–98]. These works have been reviewed and elaborated in Section 4.1.

2.2. Viscosity

The ability of a fluid to resist deformation under shear stress is measured by its viscosity [99]. The internal friction creates flow resistance between the fluid layers to varying degrees. To cite a simple instance, water is not as viscous as honey. Since viscosity directly affects pumping power and energy consumption rates, optimizing flow parameters for the industrial applications of nanofluids is a crucial characteristic. There is no unanimous agreement in the literature regarding the rheological behaviour of nanofluids as non-Newtonian or Newtonian (fluids). However, nanofluids are observed to behave as non-Newtonian fluids above low volume fractions (by 'low', we mean less than 0.02%) [100]. Researchers have studied how the temperature, base fluid viscosity, and the size, shape, and volume concentration of the nanoparticles affect the nanofluid viscosity. Several correlation-based models have been developed to predict nanofluids' viscosity. Some of these [101–105] are described in Table 2.

Table 2. A few correlation-based models for nanofluid viscosity.

Authors	Equation
Einstein, 1906 [101]	$\mu_{nf} = \mu_{bf} \left(1 + \frac{5}{2}\varphi \right)$
Andrade, 1930 [102]	$\mu_{bf} = Ae^{\frac{B}{T}}$
Batchelor, 1977 [103]	$\mu_{nf} = \mu_{bf} \left(1 + \frac{5}{2}\varphi + 6.2\varphi^2 \right)$
Bicerano et al., 1999 [104]	$\mu_{nf} = \mu_{bf} (1 + \eta\varphi + K_H\varphi^2 + \dots)$
Vajjha and Das, 2008 [105]	$\frac{\mu_{nf}}{\mu_{bf}} = A_1 e^{(A_2\varphi)}$

In the equations presented in Table 2, the symbol μ_{nf} refers to the viscosity of the nanofluid, μ_{bf} denotes the viscosity of the base fluid, φ refers to the volume fraction, and T

is the temperature. The symbols A , B , A_1 , and A_2 are empirical constants. In the equation by Bicerano et al., 1999 [104], η is a virial coefficient (called the intrinsic viscosity), and K_H is the Huggins coefficient [104]. For a detailed exposition, the reader should consult the cited references. Table 2 also shows that the relationship of nanofluid viscosity with its volumetric concentration is either a higher-order polynomial or an exponential function. In recent years, applications of AI and ML in the prediction of nanofluid viscosity have gained popularity [45,88,95,106–114], which have been discussed elaborately in Section 4.2.

2.3. Specific Heat Capacity

The SHC of a substance is the amount of thermal energy required to raise the temperature of the unit mass of any substance by one degree. Thus, a substance of high SHC will absorb more heat than an equal mass of a lower-SHC substance for the same temperature increase. This aspect becomes particularly useful in designing coolants for heat transfer applications. Specifically, the coolant should absorb a large amount of heat energy from the workpiece while not showing too much increase in temperature, as that would reduce its cooling efficiency. The AI tools like the DSC [115,116] and the MDSC [117] are typically used to assess the SHC of nanofluids.

Several factors influence the SHC in nanofluid applications, which include the volume fraction, the temperature, the base fluid type, and the type of particle used [118]. Several analytical models have been developed to determine a nanofluid's specific heat capacity. Some of these [119–121] are summarised in Table 3.

Table 3. A few correlation-based models for nanofluid specific heat capacity.

Authors	Formula
Pak et al. [119]	$C_{p,nf} = \varphi C_{p,np} + (1 - \varphi) C_{p,bf}$
Xuan et al. [120]	$C_{p,nf} = \frac{\varphi \rho_{np} C_{p,np} + (1 - \varphi) \rho_{bf} C_{p,bf}}{\varphi \rho_{np} + (1 - \varphi) \rho_{bf}}$
Sundar et al. [121]	$C_{p,hnp} = \frac{\rho_{np,1} \omega_1 + \rho_{np,2} \omega_2}{\omega_1 + \omega_2}$

In the equations presented in Table 3, $C_{p,nf}$ refers to the SHC of the nanofluid, $C_{p,np}$ refers to the SHC of the nanoparticle, and $C_{p,bf}$ denotes the SHC of the base fluid. The symbol φ is the volume fraction, ρ_{np} is the density of the nanoparticle, and ρ_{bf} is the density of the base fluid. The equation by Sundar et al. [121], as depicted in the last row of Table 3, can be used to determine the (effective) SHC of hybrid nanoparticles ($C_{p,hnp}$). In this equation, subscripts 1 and 2 refer to the different types of nanoparticles, and ω_1 and ω_2 are the weight percentages of the nanoparticles. The SHC of hybrid nanoparticles obtained from this equation can be substituted in the equations by Pak et al. [117] or Xuan et al. [120] to obtain the SHC of the hybrid nanofluid. In recent years, several models based on ML, AI, and GA methods have been developed by the researchers to predict the SHC of nanofluids [122–129]. These are discussed in detail in Section 4.3.

3. Algorithms

Various algorithms and techniques have been employed by diverse research groups in the surveyed literature. A brief overview of such algorithms is presented in the following subsections.

3.1. Artificial Neural Network

The ANNs are computational models that mimic the human brain's neural structure, providing a foundation for advancements in AI. These networks consist of interconnected nodes or neurons, which process input data and produce output, much like the biological neurons in the brain [130]. The basic structure of an ANN includes an input layer, one or more hidden layers, and an output layer [131]. Figure 2 depicts a simple ANN with an

input layer of four neurons, one hidden layer of three neurons, and an output layer of one neuron. The learning process in ANNs involves adjusting the synaptic weights, which are the parameters that determine the strength of the connection between neurons. This adjustment is typically completed using backpropagation, a method that minimizes the error in the network's output by propagating the error backward through the network [132].

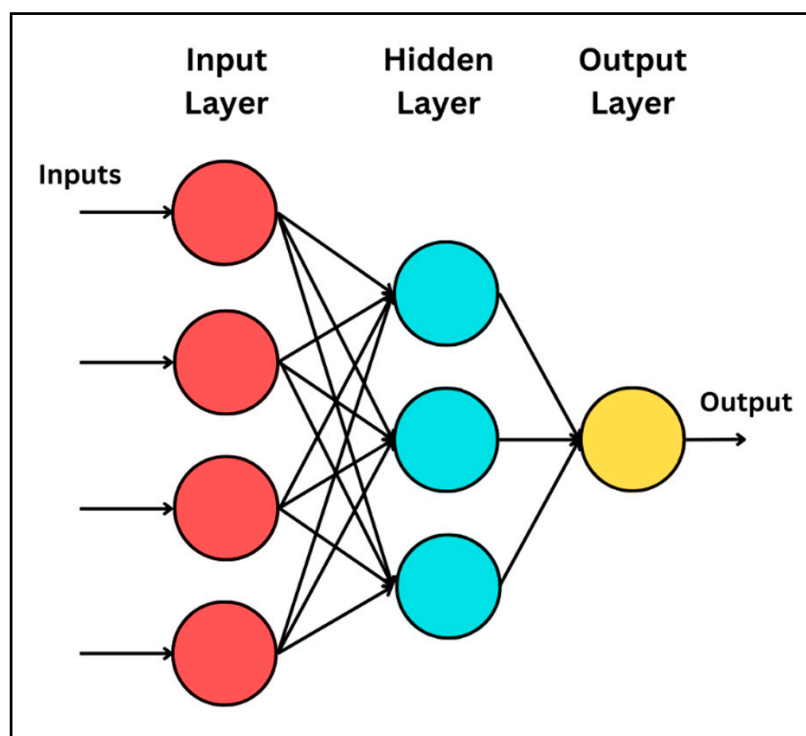


Figure 2. A simple neural network.

The most common algorithm in training ANNs is gradient descent, which iteratively adjusts weights to minimize a loss function [133]. The methodology of ANNs is applied to various tasks, which include image and speech recognition, natural language processing, and complex problem-solving in various scientific fields [132,134]. Their ability to learn from large datasets and identify data patterns makes them particularly effective for big data tasks [135].

3.1.1. RBF Neural Network

In ML, the RBF is a crucial tool used in NNs and function approximation. This real-valued function's effectiveness is derived from its dependency on the distance from a central point, which is instrumental in spatial transformations and pattern recognition. An RBF network is a feedforward network with two layers that utilize the RBF and the linear activation function in their hidden and output layers, respectively [136]. It was introduced by Broomhead and Lowe in 1988 [137]. The standout feature of RBFs is their proficiency in managing non-linear problems, attributed to their localized and radial symmetry properties. It makes them highly suitable for classification and regression tasks, where they can adeptly model complex relationships even with limited training data.

3.1.2. GMDH-Type Neural Network

The GMDH-type NN represents another significant approach in ML. Developed by Ivakhnenko in the 1960s, the GMDH is a self-organizing method that creates a model by systematically adding layers of neurons based on their correlation with the target variable [138]. This iterative process involves selecting the best neurons based on a predefined

criterion, such as the least squares method, and then combining these neurons to form a more complex structure in subsequent layers.

3.2. Support Vector Machine

The SVMs are a class of supervised learning algorithms widely used to classify and perform ML regression tasks. Introduced by Vapnik and Chervonenkis in the 1960s, SVMs gained prominence due to their robustness and efficacy in handling high-dimensional data [139,140]. The fundamental idea behind SVMs is to find a hyperplane in a high-dimensional space that distinctly classifies the data points. For linearly separable data, SVMs aim to maximize the margin between the data points of different classes, effectively finding the optimal separating hyperplane [140]. Figure 3 represents an SVM in the 2D plane for two-class classification problems. In cases where the data are not linearly separable, SVMs employ the kernel trick. This technique transforms the data into a higher-dimensional space where a separating hyperplane can be found [141].

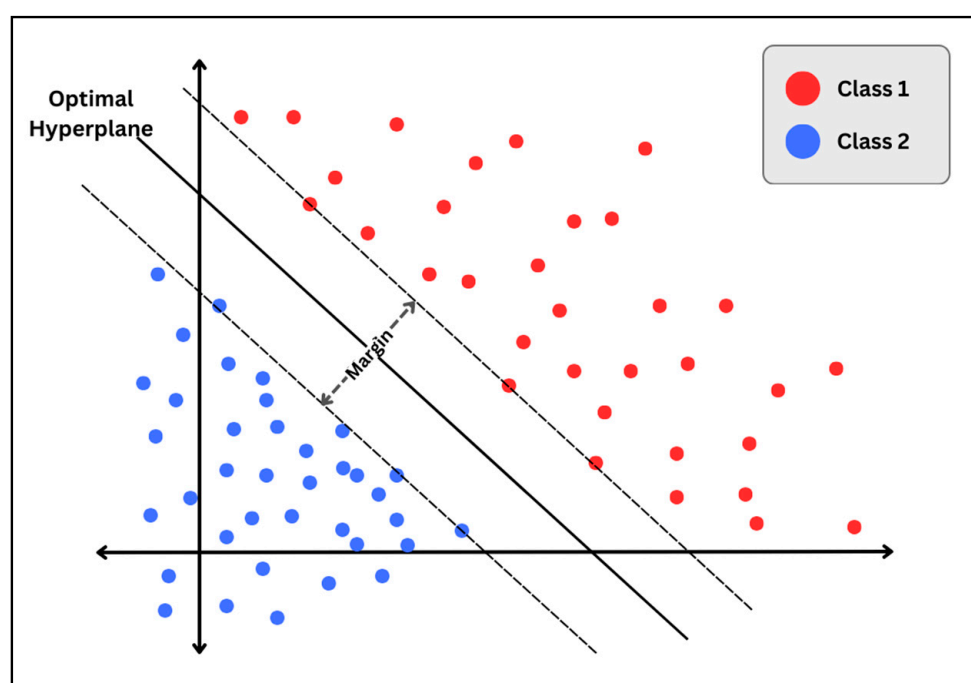


Figure 3. An SVM in 2D plane for two-class classification problem.

By incorporating the BSVR concept, SVMs expand their applicability to regression tasks [142,143]. Based on Bayesian inference principles, BSVR estimates a posterior distribution over the model parameters, providing a probabilistic interpretation of the SVM regression [144]. This approach enables the assessment of uncertainty in predictions, which is a crucial aspect in numerous real-world applications [145].

The SVMs utilize different types of kernels to accommodate various data distributions. The linear, polynomial, RBF, and sigmoid kernels are among the most common ones. Each kernel carries its strengths and is selected based on the data's nature and the specific task at hand [146]. The linear kernel is adequate for linearly separable data, while the RBF and polynomial kernels are better suited for non-linear relationships [147]. This flexibility allows SVMs to deliver strong performance across various scenarios, from simple linear separations to complex, high-dimensional classification and regression tasks. SVMs are generally renowned for their effectiveness in high-dimensional spaces and adaptability in handling diverse data types, such as text and images [148,149]. Moreover, they exhibit a reduced vulnerability to overfitting, significantly when the number of dimensions surpasses the number of samples [150].

3.3. Decision Tree

Decision Trees are a fundamental method in ML-model decisions and their possible consequences, including chance event outcomes, resource costs, and utility. The concept of decision trees is obtained from the works of Breiman et al. [151], who laid the groundwork for many current algorithms. A decision tree consists of internal nodes representing a ‘test’. Each branch depicts an outcome of the test, whereas each leaf node represents a class label. The paths from root to leaf are the classification rules [152].

One of the critical advantages of decision trees is their interpretability and simplicity. They can be visualized, which makes them easy to understand and interpret. This observation contrasts with more complex models like NNs, where the decision-making process is often opaque. However, decision trees must be more balanced, especially when dealing with complex structures and large datasets. Techniques like pruning (reducing the size of the tree), setting a minimum number of samples per leaf, or limiting the depth of the tree are often used to prevent this [151]. Several advanced techniques have been developed to extend the decision tree methodology.

3.3.1. Decision Tree Regression

This approach extends decision trees to regression problems. Instead of predicting a class, these trees predict a continuous value. The tree splits the dataset into branches, leading to terminal nodes representing that segment’s mean or median values. It is beneficial for capturing non-linear relationships in data [153].

3.3.2. Alternating Decision Tree

The ADTree is an advanced classification model that combines several weak decision trees into a more robust model. Unlike traditional decision trees, ADTrees consist of decision nodes that specify a condition and prediction nodes that provide a score. These scores are added up to make a final prediction. ADTrees are known for their interpretability and improved accuracy over single decision trees [154].

3.3.3. M5 Tree

The M5 model tree is specifically used for regression tasks. It differs from traditional regression trees by fitting linear regression models at the leaves instead of just the mean or median [155]. This allows for capturing both the hierarchical structure of the features and linear relationships among them, making M5 trees more accurate for continuous data predictions.

3.3.4. Random Forest

The RF is an ensemble learning method that builds a ‘forest’ of decision trees. Each tree in the forest is trained on a random subset of the data with replacement (bootstrap aggregating or bagging), and the final prediction is made by averaging the predictions of each tree. This approach dramatically reduces overfitting and is one of the most potent and versatile ML models available [156].

3.3.5. Extra Tree Regression

The ETRs, or Extremely Randomized Trees, are similar to the RF but introduce more randomness. When building trees, it randomly selects the cut-points for splitting nodes, which adds additional diversity to the model, often leading to improved model robustness against overfitting [157].

3.3.6. AdaBoost

The AdaBoost is an ensemble technique that builds a robust classifier by combining multiple weak classifiers, typically decision stumps (one-level trees) [158]. After each iteration, it adjusts the weights of misclassified instances, making the algorithm focus more

on complex cases in subsequent iterations. This sequential attention to the ‘hard’ parts of the training set makes AdaBoost a robust classifier.

3.3.7. Boosted Regression Tree

In this approach, regression trees are sequentially added to the ensemble, and each new tree fits the residual errors made by the previous ones. This boosting strategy focuses on areas where the previous models performed poorly, leading to improved accuracy over single models or non-boosted ensembles.

3.3.8. Gradient Boosting Machine

The GBM is a powerful ML technique for regression and classification problems, which builds an ensemble model stage-wise. It constructs new models that predict the residuals or errors of prior models and then combines them to make the final prediction. This approach allows GBMs to learn iteratively from the mistakes of previous models [159].

3.3.9. XG Boost

The gradient-boosted decision trees are designed for speed and performance. They provide a scalable and accurate solution to many supervised learning problems [160].

3.4. Genetic Algorithm

The GAs are evolutionary algorithms that mimic the process of natural selection, embodying the principles of biological evolution, to solve complex optimization and search problems. John Holland formally introduced the concept of GAs in the 1960s, and it has since been developed and refined by numerous researchers [161]. A GA operates and evolves through a cycle of stages that include selection, crossover (or recombination), and mutation. A population of candidate solutions is generated, typically represented as binary strings. The algorithm then evaluates these solutions based on a fitness function. The most fit individuals are selected to breed a new generation through crossover and mutation, introducing new genetic structures in the population [162].

One of the critical strengths of GAs is their ability to search giant, complex, and multimodal spaces where traditional optimization methods might struggle. They are particularly effective in problems where the search space is poorly understood, or the objective function is complex and non-linear [163]. GAs, however, have certain drawbacks, including the potential to converge to local optima and the difficulty in selecting the best genetic representations and fitness functions for a given problem. The MGGP is used as an extension of GA [164]. It is more reliable than the GA method, which can provide a non-linear correlation using selected operators. Like GA, the MGGP model has three leading operators (crossover, mutation, and selection). However, MGGP is a tree-based model, whereas the GA utilizes the string to represent the solutions [165].

3.5. Adaptive Neuro Fuzzy Interface

The ANFIS is a hybrid intelligent system combining NNs and fuzzy logic principles to create a framework that can capture the benefits of both in a single model. This approach was introduced by Jang in 1993 in a seminal paper that demonstrated how an NN architecture could be used to tune the parameters of a fuzzy system [166]. The core idea behind the ANFIS is to use the learning capabilities of NNs to determine the parameters of a fuzzy inference system. A fuzzy inference system uses fuzzy set theory to map inputs (features) to outputs (responses). In the ANFIS, the parameters of the fuzzy system are adjusted using methods similar to those used in NN training, such as backpropagation and least squares estimation. The ANFIS models are beneficial when the data or the relationships between variables are complex and challenging to model with traditional techniques. They have been successfully applied in control systems, pattern recognition, and prediction, where they can effectively model non-linear functions and handle uncertainty and imprecision [167].

3.6. Regression

Regression is fundamental for predicting continuous outcomes from one or more predictor variables. Its essence lies in establishing a relationship between independent variables (features) and a dependent variable (outcome) and using this relationship to predict new data points. Regression models range from simple linear forms to complex non-linear ones, each suitable for different datasets and prediction requirements. The various types of regression models used in the surveyed literature are briefly discussed below.

3.6.1. Non-Linear Regression

This form of regression is used for a complex connection between the independent and dependent variables, meaning it cannot be accurately described with a straight line. The NLR technique is essential for modelling more complex phenomena where variables interact non-linearly, such as exponential growth, logarithmic trends, or sinusoidal patterns [168].

3.6.2. Multivariate Adaptive Regression Splines

The MARS, a non-parametric regression technique, can model complex, high-dimensional datasets where relationships between variables are not easily expressible in a simple mathematical form. It is flexible and can approximate a wide variety of functional forms. The MARS methodology does this by dividing the data into segments and fitting linear regressions within them, making it adept at capturing non-linear relationships and interactions between variables [169].

3.6.3. Multivariate Polynomial Regression

This method is an extension of linear regression, where a relation of the independent and dependent variables is an n th-degree polynomial. It is helpful in cases where the linear model is too simple and inadequate. The polynomial nature allows for a more flexible curve but poses the risk of overfitting, especially with higher-degree polynomials.

3.6.4. Gaussian Process Regression

The GPR is a powerful, probabilistic non-linear modelling technique. It is beneficial in sparse data scenarios, and uncertainty estimation is crucial. The GPR technique makes predictions by placing a Gaussian process before functions, offering a flexible means to capture the underlying structure of the data. It is often used in geo-statistics, time series, and spatial data analysis [170].

A brief overview of the important AI algorithms is discussed in Table 4.

Table 4. Overview of some of the important AI algorithms.

Algorithm	Advantages	Disadvantages	Applicability
ANN	<ul style="list-style-type: none"> • Can model complex non-linear relationships. • Good for pattern recognition and classification. 	<ul style="list-style-type: none"> • Requires large datasets. • Computationally intensive. • Black box nature. 	Works well with large amounts of sample data for image and speech recognition, time series prediction, and natural language processing.
SVM	<ul style="list-style-type: none"> • Effective in high-dimensional spaces. • Memory efficient. • Versatile kernel functions. 	<ul style="list-style-type: none"> • Not suitable for large datasets. • Performs poorly with overlapping classes. 	Effective for text and hypertext categorization, image classification, and bioinformatics, especially with a clear margin of separation.

Table 4. Cont.

Algorithm	Advantages	Disadvantages	Applicability
DT	<ul style="list-style-type: none"> • Easy to understand and interpret. • Can handle both numerical and categorical data. 	<ul style="list-style-type: none"> • Prone to overfitting. • Can become unstable with small variations in data. 	Suitable for classification and regression tasks, customer segmentation, and feature selection where data can be split into clear decisions.
GA	<ul style="list-style-type: none"> • Good for searching large spaces. • Flexible and adaptable to different problems. 	<ul style="list-style-type: none"> • Can be slow to converge. • Requires careful tuning of parameters. 	Ideal for optimization problems, scheduling and planning, and machine learning parameter tuning where traditional approaches are inefficient.
ANFIS	<ul style="list-style-type: none"> • Can model complex non-linear functions. • Good interpretability compared to ANN. 	<ul style="list-style-type: none"> • Computationally intensive. • Requires expert knowledge to design the fuzzy system. 	Applicable in control systems, time series prediction, and pattern and sequence recognition where fuzzy logic can enhance model interpretability.
Regression	<ul style="list-style-type: none"> • Easy to understand and implement. • Efficient predictions. • Good for trend forecasting. 	<ul style="list-style-type: none"> • Sensitive to outliers. 	Works well in predicting sales and market trends, risk assessment in finance, and evaluating trends in data with linear relationships.

4. Application of AI for Predicting Thermophysical Properties of Nanofluids

A comprehensive review of the recent literature utilizing computational intelligence for nanofluid thermophysical property modelling has been described in the present section. Considering a diverse audience with varied technical backgrounds, this section has been preceded by a comprehensive overview of the basic concepts of nanofluid thermophysical properties (Section 2). Some essential AI algorithms used in the reviewed literature have also been discussed (Section 3). With a focus on providing valuable insights for researchers and practitioners in this rapidly evolving field, the following sections offer a detailed examination of the trends, limitations, and research gaps, alongside suggestions for future directions.

This section is divided into subsections based on a specific thermophysical property (thermal conductivity, viscosity, and specific heat capacity) and the published literature that applies AI methods for predicting that property. In addition, the results and summary of these studies have been presented in a tabular format to offer a quick overview of the key features.

4.1. Applications of AI for Predicting Thermal Conductivity of Nanofluids

Esfahani et al. [88] demonstrated that incorporating nanoparticles in MO significantly enhanced the TC of the resulting nanofluids. The predictive models, particularly the ANFIS model, showed high accuracy and reliability in estimating the TC of these nanofluids. These models aimed to predict the TC and viscosity of nanofluids, considering volume concentration and types of nanoparticles as the input factors. The paper demonstrated that the TC of nanofluids increases with the concentration of nanoparticles and that silver nanoparticles show a higher TC than titanium oxide and copper nanoparticles. The findings have underlined the potential of using such nanofluids for improved heat transfer in various applications, which include electronic cooling systems.

Although ANNs are potentially valuable tools that can approximate any function, they must provide practical insights into how the inputs relate to the output. As such, they are justifiably treated as ‘Black Box’ models. The researchers have used an innovative approach of combining fuzzy logic with ANN (i.e., ANFIS) to address this problem. It enables deriving a correlation between the inputs and outputs (TC and viscosity) from the neural network (ANFIS) models. The researchers also noted that the correlation obtained

from their AI-based models demonstrated a better agreement with experimental data when compared to the empirical equations of previous research groups [85,171].

Rostamian et al. [89] presented a comprehensive study on the TC of a CuO–SWCNTs hybrid nanofluid by combining experimental measurements with ANN modelling to predict TC changes in temperature and concentration. The experiment covered a range of temperatures (20–50 °C) and solid volume fractions (0.02% to 0.75%). The findings indicate that the ANN model offers better precision and accuracy than the correlation proposed by the authors on the same dataset.

The study by Ahmadi et al. [90] has significantly contributed to the nanofluid TC prediction field. It successfully implemented and compared three different connectionist methods. The dataset consisted of temperature in the range of (10–70 °C), nanoparticle size in the 5–282 nm range, and volumetric concentration in the 0.25–6% range. The GA–LSSVM algorithm, in particular, showed superior performance, highlighting the potential of combining GAs with LSSVM for enhanced predictive accuracy. The GA and SVM have served as novel nanofluid thermal-property-prediction approaches. In addition, the inclusion of nanoparticle size as an input parameter in the models yields a more comprehensive model that can be applied to a broader range of important factors influencing the nanofluid's thermal conductivity. However, the authors have reported a training R^2 of 0.8999 and testing R^2 of 0.7832. This difference, in our opinion, may indicate the possibility of overfitting.

The paper by Alade et al. [91] presented a comprehensive study using the SVR to model the TC enhancement of both metal and metallic oxide nanofluids. By considering various factors like the type of base fluid, nanoparticle type, and volume fraction, the authors have developed models that significantly outperform classical and empirical models. Their findings have demonstrated the versatility of SVR in handling the non-linear and complex nature of nanofluid behaviour. Specifically, the study has highlighted how the temperature and volume fraction influence TC enhancement in different classes of nanofluids, revealing critical insights for future nanofluid research and applications.

Esfe et al. [92] have provided a significant contribution to knowing the thermal properties of hybrid nanofluids through the experimental investigation of the TC of a ZnO–DWCNT/EG hybrid nanofluid across various concentrations and temperatures, achieving a maximum TC ratio of $\approx 24.9\%$ at 50 °C and 1.9% solid volume fraction. The use of an ANN for modelling these properties has showcased the potential of ML in enhancing the prediction accuracy of nanofluid thermal characteristics. The AI-based approach has demonstrated better results than the existing theoretical models [84,172,173] for all solid volume fractions.

Ahmadi et al. [93] have presented an approach to predict the TC ratio of an Al_2O_3 /EG nanofluid using the LSSVM coupled with a GA, which was introduced by Ahmadi et al. in 2018 [90] for an Al_2O_3 /water nanofluid. In this work, the dataset used had a volumetric concentration in the range of 0.2–5%, a temperature in the range of 10–70 °C, and a nanoparticle size in the range of 5–282 nm. Using the LSSVM–GA has provided an effective means to optimize the model's parameters. This has resulted in high accuracy, as evidenced by the low value of MSE and high R^2 values. The results of this study have demonstrated a significant advancement in predictive modelling for nanofluid TC, offering a comprehensive tool that accounts for crucial variables affecting the thermal behaviour of nanofluids. As evidenced by the survey, the authors have reported much better results than the previous work by Ahmadi et al. [90]. Furthermore, the training and the testing R^2 were 0.99, indicating minimal or no overfitting. However, the datasets used in both works [90,93] had similar statistics. Overfitting the Al_2O_3 dataset [90] by the same algorithm (GA–LSSVM) may indicate the presence of considerable noise in that dataset. This characteristic highlights the importance of proper data collection and pre-processing.

Akhgar et al. [94] have significantly contributed to predicting the TC in hybrid nanofluids. By developing various ANNs with different architectures and training algorithms, the study has effectively forecasted the TC of an MWCNT– TiO_2 /water–EG hybrid nanofluid.

The results demonstrate that the optimized ANN models can predict TC more accurately than traditional correlation methods.

Shahsavari et al. [95] contributed significantly to understanding how Fe₃O₄ nanoparticle concentration and temperature affect the TC of liquid paraffin-based nanofluids. Using a GMDH-type NN model to predict TC, the authors have showcased the practical application of ML techniques in complex fluid dynamics and heat transfer studies. The high accuracy of the model, as shown by the performance metrics, emphasizes the potential of such computational approaches in predicting nanofluid properties when traditional models (like the Hamilton and Crosser Model [85]) underperform at higher concentrations.

Rostami et al. [96] have performed a comprehensive study on predicting the TC of MWCNT-liquid paraffin nanofluids using ANNs. They efficiently utilized ANN to model the TC based on mass fraction and temperature. The study shows that the ANN model, particularly with six neurons in the hidden layer, yields highly accurate predictions, as evidenced by a high correlation coefficient and low value of MSE. The results indicate that ANN could be a powerful tool in forecasting the thermal behaviour of nanofluids, thereby reducing the need for extensive experimental work. However, due to the small amount of data, the authors used only 28 data points (for training and testing) and no validation dataset. The dataset was split into train and test datasets in a 7:3 ratio. When sufficient data are unavailable, techniques such as K-fold cross-validation can be used. However, for reliable prediction, the collection of adequate data is recommended.

The paper by Sharma et al. [97] has offered a comprehensive analysis of the TC prediction of TiO₂-water nanofluids using various ML algorithms. The authors used a novel approach of nanoparticle shape as an input parameter for the models. The GBM algorithm emerged as the most accurate, outperforming the other methods regarding MSE and R² values, thereby demonstrating its effectiveness in reducing errors and noise during iterative predictions. The findings of this study not only enhance the understanding of nanofluid thermal properties but also demonstrate the robust capabilities of ML algorithms in modelling complex physical phenomena such as nanofluid TC.

The paper by Sahin et al. [98] has substantially contributed to nanofluid research, particularly in predicting the TC and zeta potential of Fe₃O₄/water nanofluids using ML techniques. The ANN models for these predictions offer high accuracy, as demonstrated by low MSE and high R² values. The results show that ANN models outperform the mathematical correlation in terms of accuracy, highlighting the effectiveness of ML in the thermophysical property prediction of complex systems. However, as the study shows, more data points are needed as the authors have used just 27 data points for TC and 18 for the zeta potential. The ML models require many data points to provide reliable results. As such, efforts must be made to gather sufficient data.

The summary of the above-reviewed literature and their RMSE and R² values are presented in Table 5.

Table 5. Overview of recent work of modelling nanofluid TC using AI techniques.

Authors	Method	Nanofluid	Input Variables	MSE	R ²
Esfahani et al., 2017 [88]	ANFIS	Ag/MO	volume concentration and type of nanoparticles	3.79×10^{-4}	0.989
Esfahani et al., 2017 [88]	ANFIS	Cu/MO	'do'	2.88×10^{-4}	0.979
Esfahani et al., 2017 [88]	ANFIS	TiO ₂ /MO	'do'	2.03×10^{-4}	0.986
Rostamian et al., 2017 [89]	ANN	CuO-SWCNTs/EG water	temperature and solid volume fraction	-	-
Ahmadi et al., 2018 [90]	SVM with GA	Al ₂ O ₃ /Water	temperature, size of nanoparticles, volume concentration	5.5×10^{-4}	0.783

Table 5. Cont.

Authors	Method	Nanofluid	Input Variables	MSE	R ²
Alade et al., 2018 [91]	SVM	(Al and Cu) with water, EG, and Transformer Oil	suspension temperature, thermal conductivities of the base fluid and nanoparticles, particle size, and volume fraction	1.23	0.993
Alade et al., 2018 [91]	SVM	(Al ₂ O ₃ and CuO) with water, EG, and Transformer Oil	'do'	1.79	0.961
Esfe et al., 2018 [92]	ANN	ZnO–DWCNT in EG	nanoparticle concentration, temperature, nanoparticle composition	5.35×10^{-5}	0.99
Ahmadi et al., 2019 [93]	SVM with GA	Al ₂ O ₃ /EG	temperature, concentration of nanoparticles, and particle size	4.59×10^{-5}	0.99
Akhgar et al., 2019 [94]	ANN	MWCNT–TiO ₂ /Water–EG Hybrid Nanofluid	temperature and volume fraction	1.02×10^{-5}	-
Shahsavari et al., 2019 [95]	GMDH type NN	Fe ₃ O ₄ /paraffin	volume concentration and temperature	3.2×10^{-4}	0.96
Rostami et al., 2020 [96]	ANN	MWCNT–Paraffin	mass fraction and temperature	7.53×10^{-5}	0.993
Sharma et al., 2022 [97]	GBR	TiO ₂ /Water	temperature, volume fraction, shape, and size of nanoparticles	0.2×10^{-3}	0.99
Sharma et al., 2022 [97]	SVR	TiO ₂ /Water	'do'	0.2×10^{-1}	0.69
Sharma et al., 2022 [97]	DTR	TiO ₂ /Water	'do'	1.1×10^{-3}	0.98
Sahin et al., 2023 [98]	ANN	Fe ₃ O ₄ /Water	temperature and concentration	1.47×10^{-5}	0.997

4.2. Applications of AI for Predicting Viscosity of Nanofluids

Esfahani et al. [88] presented an in-depth analysis of the viscosity and TC of nanofluids composed of silver, copper, and titanium oxide nanoparticles dispersed in mineral-insulating oil. The researchers employed a high-pressure homogenization process without additives or surfactants. The ANFIS and non-linear regression techniques were used to develop new models based on experimental data. The study findings suggested that increasing nanoparticle concentration in the base fluid enhances the TC and viscosity, which can lead to challenges in practical applications like duct blocking and higher pressure drops in systems. The authors also noted that the AI-based models were superior compared to equations suggested by previous researchers in modelling their experimental data.

Alrashed et al. [106] presented a comprehensive study on the thermophysical properties of carbon-based nanofluids. The researchers focused on the viscosity, density, and TC of Diamond–COOH and MWCNT–COOH nanoparticles dispersed in water without surfactants or additives. Their study spanned temperatures from 20 °C to 50 °C and particle volume fractions from 0 to 0.2%. The authors compared the soft computing techniques with existing formulas and found that the soft computing methods result in lesser error than the correlation-based models. They concluded the ANN to be the best predictor model in their study, based on the MAPE value.

Esfe et al. [45] investigated the viscosity of a CuO–EG nanofluid at different concentrations and temperatures. The study utilized a GA-based NN to develop a model to predict

the nanofluid's viscosity based on experimental data. The model was trained with 36 data points and validated with 6 data points, covering a range of volume concentrations (0 to 1.5%) and temperatures (27.5 °C to 50 °C). The findings reveal that viscosity increased with volume concentration and decreased with rising temperature, with temperature having a more significant effect at lower concentrations. The best-performing ANN configuration was identified as having two hidden layers with eight neurons each. The study concluded that volume concentration is more influential on viscosity than temperature. This finding thus illustrates how AI methods can serve to comprehend the underlying physics of transport phenomena.

In their study, Esfe et al. [107] aimed to predict the rheological behaviour of an Al₂O₃-MWCNT/5W50 hybrid nano-lubricant using an ANN model. Based on experimental data, the study proposed an ANN model and a new correlation with three inputs for the ANN model: temperature, volume fraction, and shear rate. The paper demonstrated that the ANN model, which uses a maximum of thirty-five neurons in one hidden layer, could predict the relative viscosity of the nano-lubricant more accurately than the empirical correlation. The ANN models demonstrated a maximum margin of deviation of ≈0.07%, while empirical correlations had a maximum margin of deviation of ≈7.3%.

Demirpolat and Das [108] investigated the viscosity of CuO nanofluids at various pH values and temperatures using different AI methods, specifically the ADTree and MLP, with the MLP performing better than the ADTree. The researchers found that the viscosity of nanofluids increased with the pH value but decreased with rising temperature. This study is significant in creating predictive models based on different computational intelligence techniques to predict the viscosity of nanofluids at a different pH.

Shahsavari et al. [95] focused on assessing the impacts of Fe₃O₄ nanoparticle concentration and temperature on the viscosity and TC of a liquid paraffin-based nanofluid. The study conducted experiments with Fe₃O₄ concentrations, ranging from 0.5 to 3% and temperatures from 20 °C to 90 °C, using oleic acid as a surfactant. It can be noted that the nanofluid exhibits shear-thinning behaviour (steady, non-Newtonian fluid behaviour characterized by an apparent viscosity that decreases with increasing shear rates), and both its viscosity and TC increased with nanoparticle concentration. However, the viscosity decreased with increased temperature, while TC increased. An ANN, specifically a GMDH-type NN, was employed to model these properties using the experimental data. The results indicated that the model could estimate outputs with low error and high R² values.

Ghaffarkhah et al. [109] investigated the dynamic viscosity of four distinct hybrid nano-lubricants. The base fluid consisted of SAE 40 engine oil, while the nanoparticles comprised 80-volume percentage oxide nanoparticles (SiO₂, Al₂O₃, MgO, and ZnO) and 20-volume percentage COOH-functionalized MWCNTs. Temperatures ranging from 25–50 °C and solid volume fractions of 0.05, 0.25, 0.50, 0.75, and 1% were used for the tests. The paper uses DT, RF, SVM, and RBF-ANN to predict nanofluid viscosity, with DT and SVM techniques showing superior accuracy. The ML models outperformed the empirical models [103,174,175] used to predict the dynamic viscosity of nanofluids. The authors used an innovative approach of using data from four different types of COOH-functionalized MWCNTs-based nanoparticles, making their model more robust and generalizable than studies that used only one type of nanoparticle. Unfortunately, each of the four types of nanoparticles had only 30 data points. This issue of data size remains to be addressed.

Toghraie et al. [110] focused on developing an ANN model to predict the viscosity of a silver/EG nanofluid. The study involved creating an experimental dataset by measuring the viscosity of the nanofluid at different temperatures and nanoparticle concentrations. This dataset was then used to train and test the ANN model. The researchers found that the ANN model could predict the viscosity with high precision, outperforming traditional correlation methods. However, only 42 data points were used, and a larger sample size was required.

Ahmadi et al. [111] performed an in-depth study focusing on applying different ML methods to predict the dynamic viscosity of a CuO/water nanofluid. The ML models used

in the study include the MPR, the MARS, the ANN-MLP, the GMDH, and the M5-tree. This study concluded that the ANN is the most reliable approach for modelling nanofluid viscosity. The authors used data from various experimental studies to apply their model to multiple inputs. The authors used temperature concentration and nanoparticle size as inputs, as the importance of these variables has been pointed out by previous literature. The study's significance lies in its attempt to understand the relative importance of these variables. The authors found concentration to be the most influential, while nanoparticle size was the least influential.

Gholizadeh et al. [112] presented a novel application of the Random Forest method to accurately estimate Newtonian nanofluids' viscosity. The research is significant for using RF in this context for the first time, aiming to enhance the accuracy and reliability in predicting nanofluids' thermophysical properties. In their study, the RF performs better than ANN, SVR, and all the correlation-based models used in their research. In addition, the authors conducted a comparative trend evaluation to validate the predictive accuracy and robustness of their proposed AI-based models in comparison to the available correlation-based models for estimation of the relative viscosity of various nanofluids, including SiO₂/DI-Water, Al₂O₃/EG-water (20:80), ZnO/water and CuO/EG-water. The authors used a sufficiently large dataset comprising 2890 data points. However, the results are only satisfactory for RF. This fact may be due to the data scaling method used. Scaling the input is often essential for a good performance of ML models, but the scaling method can considerably affect the performance. The authors scaled the input data between 0 and 1 based on the dataset's minimum and maximum data values. This type of scaling, also known as Min–Max Scaling, is sensitive to outlier data points. We recommend Standard Scaling, which uses the mean and standard deviation of the dataset to scale the data. It is less sensitive to outliers and can improve the performance of the ML models. Nevertheless, the study concluded that the AI models (especially RF) yield better predictive accuracy when compared to the existing empirical and theoretical correlations.

Kanti et al. [113] explored the viscosity properties of fly ash nanofluids and fly-ash–Cu hybrid nanofluids. The research is significant for using advanced and novel computational algorithms like the MGGP to predict and optimize the dynamic viscosity of these nanofluids based on experimental data.

Dai et al. [114] explored the application of ML techniques, specifically the GPR with different covariance functions, to predict the dynamic viscosity and torque of SiO₂ nanoparticles in EG base fluid. This study presented a comprehensive approach to utilizing advanced ML models to understand and predict the rheological properties of nanofluids and reported low error and high R² values. Based on available data, the authors used a dataset with only 45 data points for dynamic viscosity and 208 data points for torque prediction. However, the authors employed the K-fold cross-validation technique to overcome the problems associated with small datasets. Nevertheless, the need for sufficient data cannot be ignored for ML models to work reliably, and 45 data points are insufficient.

The summary of the above-reviewed literature and their RMSE and R² values are presented in Table 6.

Table 6. Overview of recent work of modelling nanofluid viscosity using AI techniques.

Authors	Method	Nanofluid	Input Variables	MSE	R ²
Esfahani et al., 2017 [88]	ANFIS	Ag/MO	volume concentration of nanoparticles and the type of nanoparticles	2.21×10^{-5}	0.977
Esfahani et al., 2017 [88]	ANFIS	Cu/MO	'do'	3.84×10^{-5}	0.999
Esfahani et al., 2017 [88]	ANFIS	TiO ₂ /MO	'do'	1.02×10^{-5}	0.998
Alrashed et al., 2018 [106]	NLR	MWCNT-COOH/water	temperature and volume fraction	7.36×10^{-5}	-
Alrashed et al., 2018 [106]	NLR	Diamond-COOH/water	'do'	8.24×10^{-4}	-
Alrashed et al., 2018 [106]	ANN	MWCNT-COOH/water	'do'	3.89×10^{-5}	-
Alrashed et al., 2018 [106]	ANN	Diamond-COOH/water	'do'	8.5×10^{-4}	-
Alrashed et al., 2018 [106]	ANFIS	MWCNT-COOH/water	'do'	1.84×10^{-8}	-
Alrashed et al., 2018 [106]	ANFIS	Diamond-COOH/water	'do'	7.47×10^{-4}	-
Esfe et al., 2018 [45]	GA-ANN	CuO/EG	volume concentration and temperature	-	0.999
Esfe et al., 2018 [107]	ANN	Al ₂ O ₃ -MWCNT/5W50	temperature, volume fraction, and shear rate	0.7×10^{-6}	0.999
Demirpolat and Das, 2019 [108]	ADTree	CuO/(water + ethanol + EG)	Reynolds number, pH, nanoparticle percentage, nanofluid temperature, nanofluid density, and average speed of nanofluids	5.6×10^{-2}	-
Demirpolat and Das, 2019 [108]	MLP	'do'	'do'	2.3×10^{-2}	-
Shahsavari et al., 2019 [95]	GMDH-NN	Fe ₃ O ₄ /liquid paraffin	nanoparticle concentration, temperature, and shear rate	3.24×10^{-6}	0.96
Ghaffarkhah et al., 2019 [109]	DT	80 Vol% (SiO ₂ , Al ₂ O ₃ , MgO, and ZnO) + 20 Vol% COOH-functionalized MWCNTs/SAE 40 Engine oil	temperature and solid volume fraction	-	-
Ghaffarkhah et al., 2019 [109]	RBF-ANN	'do'	'do'	-	-
Ghaffarkhah et al., 2019 [109]	RF	'do'	'do'	-	-
Ghaffarkhah et al., 2019 [109]	SVM	'do'	'do'	-	-
Toghraie et al., 2019 [110]	ANN	Ag/EG	temperature and volume fraction of nanoparticles	6.96×10^{-5}	-

Table 6. Cont.

Authors	Method	Nanofluid	Input Variables	MSE	R ²
Ahmadi et al., 2020 [111]	ANN	CuO/water	size, temperature, and concentration of the nanoparticles	5.6×10^{-4}	0.999
Ahmadi et al., 2020 [111]	GMDH	CuO/water	'do'	6.5×10^{-4}	0.999
Ahmadi et al., 2020 [111]	MARS	CuO/water	'do'	1.4×10^{-3}	0.999
Ahmadi et al., 2020 [111]	M5-Tree	CuO/water	'do'	1.22×10^{-2}	0.995
Ahmadi et al., 2020 [111]	MPR	CuO/water	'do'	1.63×10^{-2}	0.994
Gholizadeh et al., 2020 [112]	RF	Various nanofluids ¹	temperature, solid volume fraction, viscosity of the base fluid, nanoparticle size, and density of nanoparticles	1.92×10^{-2}	0.978
Gholizadeh et al., 2020 [112]	MLP	Various nanofluids ¹	'do'	1.42×10^{-1}	0.837
Gholizadeh et al., 2020 [112]	SVR	Various nanofluids ¹	'do'	9.2×10^{-2}	0.885
Kanti et al., 2021 [113]	MGGP	(Fly ash)/water	concentration range and temperature range of nanofluids	3.61×10^{-6}	0.999
Kanti et al., 2021 [113]	MGGP	(Fly-ash–Cu)/water	'do'	3.97×10^{-5}	0.995
Kanti et al., 2021 [113]	ANN	(Fly ash)/water	'do'	3.17×10^{-6}	0.999
Kanti et al., 2021 [113]	ANN	(Fly-ash–Cu)/water	'do'	1.16×10^{-5}	0.999
Dai et al., 2023 [114]	GPR	SiO ₂ /EG	volume fraction, shear rate, and temperature	5.76×10^{-2}	0.996

¹ Al₂O₃/(water, DI water, EG, EG/water, TO, polyalphaolefins), SiO₂/(EG, DI water, ethanol, EG/water (30:70), water), TiO₂/(water, EG, DI water, EG/water), CuO/(water, EG, EG/water), ZnO/(water, EG), MgO/EG, Fe₃O₄/(water, toluene), Mg(OH)₂/EG, Co₃O₄/EG, SiC/DI water, diamond/(water, EG/water), CNTs/(water, EG), MWCNT–COOH/water, Ce₂/EG.

4.3. Applications of AI for Predicting Specific Heat Capacity of Nanofluids

Alade et al. [122] focused on developing a highly accurate model for predicting the SHC of alumina/ethylene glycol nanofluids. This work is significant for proposing a novel technique for more precise and reliable calculation of the efficiency of solar collectors. The authors of this article proposed a BSVR model, which was trained using 84 experimental datasets and validated with 17 test sets. The model demonstrated remarkable accuracy, outperforming existing theoretical models [119,120]. This paper's use of the Bayesian optimization algorithm to find the optimal hyperparameters was noteworthy as it simplifies discovering the optimal model architecture. However, the number of data points (101) should be increased for a more reliable prediction.

Hassan and Banerjee [123] presented a novel application of ML techniques to estimate the SHC of molten nitrate salt-based nanofluids (with titania, alumina, and silica nanoparticles). Trained and tested on a dataset incorporating factors like temperature and nanoparticle mass fraction, the MLP-ANN model has shown a high prediction accuracy. The ANN model yields a maximum error of approximately $\approx 2\%$ and has outperformed classical analytical models [119,120], which showed an error of up to $\approx 24\%$. The study is significant because the authors trained and compared a huge number (1920) of ANN architectures by varying the number of neurons (between 5 and 100), 12 different activation functions, and different weight optimization algorithms. The training of such networks is time-consuming, and the authors experimented with several small datasets to determine the optimal number of data points to obtain a good prediction. They concluded it to be around 300.

Alade et al. [124] focused on developing ML models for predicting the SHC of CuO/water nanofluids. Their study employed SVR and ANN models and experimental data, including the SHC of CuO nanoparticles, their volume fractions (0.4% to 2%), and fluid temperature (293–338 K). The study revealed that the SVR model slightly outperformed the ANN model in accuracy. However, both models demonstrated superior prediction performance for the SHC of CuO/water nanofluids compared to existing theoretical models [119,120], thereby highlighting the effectiveness of ML approaches in this domain.

Daneshfar et al. [125] explored the determination of the specific heat capacity of nanofluids using various ML models. The study employed MLP-ANN, SGB tree, RBF-NN, and the ANFIS models. These models were assessed based on input parameters like nanoparticle concentration, critical temperature, operational temperature, acentric factor, and molecular weight of pure ionic liquids. The SGB model outperformed the others in accuracy and generalizability, demonstrating its applicability to unseen conditions and offering a cost-effective alternative to experimental methods. The authors used 429 training data points and 142 testing data points. They used Min-Max Scaling, but in our opinion, that is sufficient because the authors already analyzed the dataset to determine outliers and found most data points to be localized in a 'reliable zone' [125].

Adun et al. [126] investigated the SHC of water-based $\text{Fe}_3\text{O}_4\text{-Al}_2\text{O}_3\text{-ZnO}$ ternary hybrid nanofluids in three different mixture ratios of $\text{Fe}_3\text{O}_4\text{-Al}_2\text{O}_3\text{-ZnO}$: 1:1:1, 1:2:1, and 1:1:2 at various volume fractions (0.5%, 0.75%, 1%, and 1.25%). The experiments were conducted in a temperature range of 25–65 °C. The findings revealed a linear effect of temperature on the SHC of the ternary hybrid nanofluid and a decrease in SHC with increasing volume concentration. The maximum increment in SHC was observed at 1.25% volume concentration and 25 °C temperature, with the 1:1:1 mixture ratio showing the 'peaking effect' and the 1:2:1 ratio showing the lowest SHC values. The ML models (ANN and GA-SVR) and corresponding correlations were developed based on the SHC data. The SVR model outperformed the correlation-based model. In addition, the SVR showed a maximum deviation of $\approx 0.2\%$ from the experimental results, while the correlation-based model showed a maximum deviation of $\approx 12.467\%$.

Jamei et al. [127] examined the determination of SHC of molten (nitrate) salt-based nanofluids. The study developed two modern ensemble ML models, the ETR and the

AdaBoost Regression, along with RF and BRT models. The dataset included variables such as solid mass fraction, temperature, SHC of base fluid, mean diameter, and density of nanoparticles as the input parameters. The authors found that the ML models demonstrated higher predictive accuracy; in particular, the ETR model outperformed the other models in the study. This work used a sufficiently large dataset comprising 2384 data points. The authors also employed feature selection techniques, which often become necessary when working with large and complicated datasets.

Zhang and Xu [128] explored the application of GPR to model the SHC of nanofluids. Their research indicated that the SHC of nanofluids could either increase or decrease with nanoparticle concentration, showing contradictory trends in different studies. This work developed a model with data on nanofluids containing CuO and Al₂O₃ nanoparticles in water and EG, which, when applied to various compositions and temperatures, offered fast and low-cost estimations of SHC.

Said et al. [129] focused on evaluating the SHC of nanofluids using three ML models: the GPR, the XGBoost, and the SVM. The study utilized metal oxide multiwall carbon nanotubes–water nanofluids and considered various factors influencing the SHC, such as volume concentrations, temperature range, base fluid’s SHC, nanofluid density, base fluid density, and average nanoparticle diameter. The findings showed that all three models predict the SHC of hybrid nanofluids with high precision, which made them viable alternatives to traditional experimental methods. Among the three, the XGBoost model exhibited superior prediction performance.

The summary of the above-reviewed literature and their RMSE and R² values are depicted in Table 7 (see below).

Table 7. Overview of recent work of modelling nanofluid SHC using AI techniques.

Authors	Method	Nanofluid	Input Variables	MSE	R ²
Alade et al., 2019 [122]	BSVR	Al ₂ O ₃ /EG	volume fraction, temperature, SHC of nanoparticles and SHC of EG	2.2×10^{-5}	0.999
Hassan and Banerjee, 2019 [123]	ANN	(Al ₂ O ₃ , SiO ₂ , TiO ₂)/Molten Salt (KNO ₃ + NaNO ₃)	temperature and mass fraction	6.593×10^{-2}	0.999
Alade et al., 2020 [124]	BSVR	CuO/water	SHC of nanoparticles, fluid temperature, volume fraction	5.29×10^{-6}	0.999
Alade et al., 2020 [124]	ANN	CuO/water	‘do’	6.25×10^{-6}	0.999
Daneshfar et al., 2020 [125]	MLP-ANN	Al ₂ O ₃ /IL	nanoparticle concentration, critical temperature, operational temperature, acentric factor, and molecular weight of pure ionic liquids	1.32×10^{-2}	0.943
Daneshfar et al., 2020 [125]	ANFIS	Al ₂ O ₃ /IL	‘do’	3.2×10^{-2}	0.875
Daneshfar et al., 2020 [125]	RBF-ANN	Al ₂ O ₃ /IL	‘do’	2.01×10^{-2}	0.92
Daneshfar et al., 2020 [125]	SGB tree	Al ₂ O ₃ /IL	‘do’	2.49×10^{-3}	0.987
Adun et al., 2021 [126]	ANN	Fe ₃ O ₄ -Al ₂ O ₃ -ZnO/water	temperature, volume concentration, and mixture ratio	480.4338	0.942
Adun et al., 2021 [126]	GA-SVR	‘do’	‘do’	89.69037	0.997
Jamei et al., 2021 [127]	ETR	Molten salt (nitrate)-based nanofluids	solid mass fraction, temperature, SHC of base fluid, mean diameter, and density of nanoparticles	2.42×10^{-2}	0.993

Table 7. Cont.

Authors	Method	Nanofluid	Input Variables	MSE	R ²
Jamei et al., 2021 [127]	ABR	'do'	'do'	3.44×10^{-2}	0.990
Jamei et al., 2021 [127]	RF	'do'	'do'	5.41×10^{-2}	0.984
Jamei et al., 2021 [127]	BRT	'do'	'do'	6.29×10^{-2}	0.981
Zhang and Xu, 2021 [128]	GPR	(Al ₂ O ₃ ,CuO)/(water EG)	temperature, SHCs of nanoparticles and base liquids, and nanoparticle volume concentrations	3.61×10^{-6}	0.999
Said et al., 2022 [129]	GPR	(metal oxide + MWCNT)/water	volume concentration, temperature range, SHC of base fluid, nanofluid density, base fluid density, and average nanoparticle diameter	54.06	0.995
Said et al., 2022 [129]	XGBoost	(metal oxide + MWCNT)/water	'do'	98.13	0.995
Said et al., 2022 [129]	SVM	(metal oxide + MWCNT)/water	'do'	97.97	0.990

Figure 4 presents the number of publications on thermophysical property research of nanofluids with AI techniques (such as ML and GA), as acquired from the Scopus database. As outlined above, the survey indicates that the number of research publications on nanofluid TC and viscosity (concerned with applying AI techniques) far exceeds the number of articles devoted to AI applications on SHC.

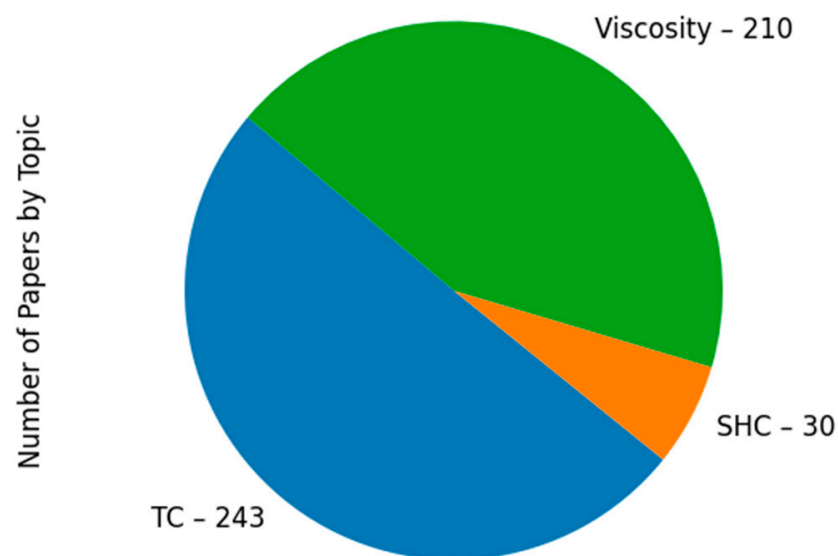


Figure 4. Pie chart representing the number of papers by topic retrieved from Scopus database (information available on 25 February 2024).

5. Conclusions and Future Scope

The present review focuses on a comprehensive overview of the recent literature on the application of AI techniques in nanofluids, particularly the prediction of thermophysical properties of nanofluids: the TC, the viscosity, and the SHC. An extensive literature analysis shows that the computational intelligence applications in this domain have steadily increased over the past decade, with researchers using varied techniques on

various nanofluids. Given the nanofluids' vast potential to replace traditional heat transfer fluids and coolants in machinery, this offers exciting novel avenues.

- i. One of the noteworthy findings of our review is the consistent superiority of AI-based models over traditional theoretical and correlation-based approaches in predicting the thermophysical properties of nanofluids. These theoretical models often exhibit uncertainties and fail to predict experimental results precisely, limiting their practical applications [91,176,177]. As outlined in the previous sections, the utilization of machine learning algorithms has yielded a more accurate estimation of the properties of NFs due to their ability to effectively map non-linear relationships between input and output variables [126]. Not only do these models offer higher accuracy, but they also present a more accessible and cost-effective alternative to experimental methods.
- ii. Furthermore, our review underscores the vast potential of nanofluids to revolutionize heat transfer fluids and coolants in various applications. However, nanofluid thermophysical properties exhibit non-linear relationships and are challenging to model using traditional theoretical models, while conducting experimental measurements is time-consuming, labour-intensive, and costly. In this scenario, AI techniques like ML become useful. ML extracts patterns and knowledge from given data without first principles, introducing a new paradigm: 'use data to discover, rather than validate, new hypotheses and models' [178]. Integrating big data and machine learning is transforming various industries, including multiphysics research, leveraging high-quality data from improved experimental and simulation studies and archival data. By harnessing AI techniques to predict the complex relation governing nanofluid thermophysical properties, researchers are paving the way for innovative thermal and energy systems solutions for industrial applications like solar collectors, heat exchangers, and PV/T systems [176].
- iii. However, data availability is a specific challenge related to applying AI methods in nanofluid thermophysical property prediction. For instance, the ML models are specific to the dataset they are trained on. For example, an ML model trained on the prediction of SHC of CuO/EG nanofluid in a plate heat exchanger would only be able to predict the SHC of CuO/ethylene glycol nanofluids and not of other nanofluids. It would also work only for plate heat exchangers rather than other configurations. This limits the applicability of ML models. If one desires a model that can predict the SHC of different nanofluids, the nanofluid/nanoparticle type should also be used as an additional input to the model. Among the papers reviewed, only the work by Esfani et al. [88] used nanoparticle type as an input parameter. This aspect highlights the substantial scope of research in this domain. However, incorporating nanoparticle type and other parameters in the input may increase the complexity of the dataset. As the complexity of the dataset increases, it becomes necessary to include more and more data points to obtain a good fit and avoid over-fitting, which is often not feasible due to the limitations of data availability and constraints of computational resources, which are necessary to run complex AI models. In such situations, dimensionality reduction techniques such as the Principal Component Analysis and the Linear Discriminant Analysis may be employed to reduce the dimensionality of the dataset. In addition, it must be borne in mind that the prediction models may not fully consider external factors such as impurities, contaminants, or changes in operational conditions. Moreover, the sensitivity of specific algorithms to hyperparameter settings may also impact the robustness and reliability of predictions.
- iv. Data availability is another issue that could hinder the progress of nanofluid research using AI. AI techniques such as ML require large amounts of data, and the absence of such data can seriously affect the models. Most of the reviewed work in this study has used relatively small datasets. Applying complex algorithms like the ANN on small datasets can result in overfitting, significantly reducing the predictions' reliability. For this reason, a large amount of quality data is necessary. Experimental methods and

computer-based simulations can generate these datasets. However, such exercises are liable to be expensive and time-consuming for individual research groups. However, once sufficient data are generated and made available globally in the public domain by researchers, these can be used to develop robust and powerful AI models to charter futuristic applications in efficient thermal management.

- v. It is worth noting that while thermal conductivity and viscosity have been extensively studied, the SHC of nanofluids still needs to be explored. Figure 4 presents the number of publications on nanofluid thermophysical property research with AI techniques such as ML and GA acquired from the Scopus database (as of 25 February 2024). Research on nanofluid TC with AI techniques has resulted in 243 publications; on viscosity, it has yielded 210 publications. However, just 30 published articles are devoted to applying AI techniques to the SHC of nanofluids. This trend may be attributed to the fact that, while TC and viscosity are primary thermophysical properties of any heat transfer medium, SHC considerations are relatively unimportant in applications where phase changes can be neglected. However, several researchers have pointed out the importance of SHC in enhancing the heat transfer properties of nanofluids [129,179]. Based on the preceding statistics, paying more attention to the SHC of nanofluids becomes imperative. This presents an exciting avenue for future research endeavours.
- vi. Applying AI, ML, and GA techniques in nanofluid research is still a relatively nascent field with steady academic and research interest growth. Several researchers [45,90,93] have demonstrated innovative approaches by combining metaheuristic techniques like GA with traditional ML models such as ANN and SVM, creating more robust models. This field of study is expected to grow even more in the coming years, with more and more researchers contributing to this field.

Funding: This research received no external funding.

Conflicts of Interest: The authors declare no conflict of interest.

Abbreviations

AdaBoost	adaptive boosting
ADTree	alternating decision tree
AI	artificial intelligence
ANFIS	adaptive neuro-fuzzy interface system
ANN	artificial neural network
BRT	boosted regression tree
BSVR	Bayesian support vector regression
CNT	Carbon nanotube
DI	diamond
DSC	differential scanning calorimeter
DTR	decision tree regression
EG	ethylene glycol
ETR	extra tree regression
GA	genetic algorithm
GBM	gradient boosting machine
GMDH	group method of data handling
GPR	Gaussian process regression
IL	ionic liquid
LSSVM	least square support vector machine
MAE	mean absolute error
MARS	multivariate adaptive regression splines
MDSC	modulated differential scanning calorimeter
MGGP	multi-gene genetic programming
ML	machine learning

MLP	multi-layer perceptron
MO	mineral oil
MPR	multivariable polynomial regression
MWCNT	multi-walled carbon nanotube
NLR	non-linear regression
NN	neural network
PV/T	photovoltaic/thermal
RBF-NN	radial basis function neural network
RBF	radial basis function
RF	random forest
RMS	root mean square
RMSE	root mean square error
RSM	response surface methodology
SGB	stochastic gradient boosting
SHC	specific heat capacity
SVM	support vector machine
SVR	support vector regression
TC	thermal conductivity
XGBoost	extreme gradient boosting

References

- Rosenzweig, R. *Ferrohydrodynamics*; Cambridge: New York, NY, USA, 1985; pp. 57–59. Available online: <https://books.google.co.in/books?id=Vv-1QgAACAAJ> (accessed on 31 December 2023).
- Akoh, H.; Tsukasaki, Y.; Yatsuya, S.; Tasaki, A. Magnetic properties of ferromagnetic ultrafine particles prepared by vacuum evaporation on running oil substrate. *J. Cryst. Growth* **1978**, *45*, 495–500. [[CrossRef](#)]
- Choi, S.U.; Eastman, J.A. *Enhanced Heat Transfer Using Nanofluids*; Technical Report; Argonne National Lab. (ANL): Argonne, IL, USA, 2001. Available online: <https://www.osti.gov/servlets/purl/196525> (accessed on 31 December 2023).
- Lee, S.W.; Park, S.D.; Bang, I.C. Critical heat flux for CuO nanofluid fabricated by pulsed laser ablation differentiating deposition characteristics. *Int. J. Heat Mass Transf.* **2012**, *55*, 6908–6915. [[CrossRef](#)]
- Kim, H.J.; Bang, I.C.; Onoe, J. Characteristic stability of bare Au-water nanofluids fabricated by pulsed laser ablation in liquids. *Opt. Lasers Eng.* **2009**, *47*, 532–538. [[CrossRef](#)]
- Lo, C.-H.; Tsung, T.-T.; Lin, H.-M. Preparation of silver nanofluid by the submerged arc nanoparticle synthesis system (sans). *J. Alloys Compd.* **2007**, *434–435*, 659–662. [[CrossRef](#)]
- Lo, C.-H.; Tsung, T.-T.; Chen, L.-C. Shape-controlled synthesis of Cu-based nanofluid using submerged arc nanoparticle synthesis system (sans). *J. Cryst. Growth* **2005**, *277*, 636–642. [[CrossRef](#)]
- Prasher, R.; Phelan, P.E.; Bhattacharya, P. Effect of aggregation kinetics on the thermal conductivity of nanoscale colloidal solutions (nanofluid). *Nano Lett.* **2006**, *6*, 1529–1534. [[CrossRef](#)] [[PubMed](#)]
- Muthukumar, T.; Gnanaprakash, G.; Philip, J. Synthesis of stable magnetic nanofluids of different particle sizes. *J. Nanofluids* **2012**, *1*, 85–92. [[CrossRef](#)]
- Zhu, H.; Zhang, C.; Tang, Y.; Wang, J.; Ren, B.; Yin, Y. Preparation and thermal conductivity of suspensions of graphite nanoparticles. *Carbon* **2007**, *45*, 226–228. [[CrossRef](#)]
- Kao, M.; Lo, C.; Tsung, T.; Wu, Y.; Jwo, C.; Lin, H. Copper-oxide brake nanofluid manufactured using arc-submerged nanoparticle synthesis system. *J. Alloys Compd.* **2007**, *434–435*, 672–674. [[CrossRef](#)]
- Philip, J.; Shima, P.D.; Raj, B. Nanofluid with tunable thermal properties. *Appl. Phys. Lett.* **2008**, *92*, 043108. [[CrossRef](#)]
- Yu, W.; Xie, H. A Review on nanofluids: Preparation, stability mechanisms, and applications. *J. Nanomater.* **2012**, *2012*, 435873. [[CrossRef](#)]
- Hernandez, R. Polymer gels with magnetic nanoparticles. applications in magnetic hyperthermia. polysolvat-9. In Proceedings of the 9th International IUPAC Conference on Polymer-Solvent Complexes & Intercalates, Kiev, Ukraine, 11–14 September 2012.
- Yang, D.; Yang, F.; Hu, J.; Long, J.; Wang, C.; Fu, D.; Ni, Q. Hydrophilic multi-walled carbon nanotubes decorated with magnetite nanoparticles as lymphatic targeted drug delivery vehicles. *Chem. Commun.* **2009**, *29*, 4447–4449. [[CrossRef](#)] [[PubMed](#)]
- Taylor, R.A.; Otanicar, T.; Rosengarten, G. Nanofluid-based optical filter optimization for PV/T systems. *Light Sci. Appl.* **2012**, *1*, e34. [[CrossRef](#)]
- Mahendran, V.; Philip, J. Naked eye visualization of defects in ferromagnetic materials and components. *NDT E Int.* **2013**, *60*, 100–109. [[CrossRef](#)]
- Dudda, B.; Shin, D. Effect of nanoparticle dispersion on specific heat capacity of a binary nitrate salt eutectic for concentrated solar power applications. *Int. J. Therm. Sci.* **2013**, *69*, 37–42. [[CrossRef](#)]

19. Mahian, O.; Kianifar, A.; Kalogirou, S.A.; Pop, I.; Wongwises, S. A review of the applications of nanofluids in solar energy. *Int. J. Heat Mass Transf.* **2013**, *57*, 582–594. [[CrossRef](#)]
20. Wang, Z.; Wu, Z.; Han, F.; Wadsö, L.; Sundén, B. Experimental comparative evaluation of a graphene nanofluid coolant in miniature plate heat exchanger. *Int. J. Therm. Sci.* **2018**, *130*, 148–156. [[CrossRef](#)]
21. Bigdeli, M.B.; Fasano, M.; Cardellini, A.; Chiavazzo, E.; Asinari, P. A review on the heat and mass transfer phenomena in nanofluid coolants with special focus on automotive applications. *Renew. Sustain. Energy Rev.* **2016**, *60*, 1615–1633. [[CrossRef](#)]
22. Ijam, A.; Saidur, R. Nanofluid as a coolant for electronic devices (cooling of electronic devices). *Appl. Therm. Eng.* **2012**, *32*, 76–82. [[CrossRef](#)]
23. Leong, K.; Saidur, R.; Kazi, S.; Mamun, A. Performance investigation of an automotive car radiator operated with nanofluid-based coolants (nanofluid as a coolant in a radiator). *Appl. Therm. Eng.* **2010**, *30*, 2685–2692. [[CrossRef](#)]
24. Raj, C.P.C.; Surendran, S.A.; Amjathkhan, B.; Metilda, J.B.; Devaraj, S.; Aristotle, E. Nano fluids for improving efficiency in wind turbine cooling system. *Adv. Mater. Res.* **2014**, *984*, 784–791. [[CrossRef](#)]
25. Goel, N.; Taylor, R.A.; Otanicar, T. A review of nanofluid-based direct absorption solar collectors: Design considerations and experiments with hybrid pv/thermal and direct steam generation collectors. *Renew. Energy* **2020**, *145*, 903–913. [[CrossRef](#)]
26. de Risi, A.; Milanese, M.; Colangelo, G.; Laforgia, D. High efficiency nanofluid cooling system for wind turbines. *Therm. Sci.* **2014**, *18*, 543–554. [[CrossRef](#)]
27. Rostamzadeh, H.; Rostami, S. Performance enhancement of waste heat extraction from generator of a wind turbine for freshwater production via employing various nanofluids. *Desalination* **2019**, *478*, 114244. [[CrossRef](#)]
28. Narei, H.; Ghasempour, R.; Noorollahi, Y. The effect of employing nanofluid on reducing the bore length of a vertical ground-source heat pump. *Energy Convers. Manag.* **2016**, *123*, 581–591. [[CrossRef](#)]
29. Diglio, G.; Roselli, C.; Sasso, M.; Channabasappa, U.J. Borehole heat exchanger with nanofluids as heat carrier. *Geothermics* **2018**, *72*, 112–123. [[CrossRef](#)]
30. Daneshpour, M.; Rafee, R. Nanofluids as the circuit fluids of the geothermal borehole heat exchangers. *Int. Commun. Heat Mass Transf.* **2017**, *81*, 34–41. [[CrossRef](#)]
31. Karami, M.; Akhavan-Bahabadi, M.; Delfani, S.; Raisee, M. Experimental investigation of CuO nanofluid-based direct absorption solar collector for residential applications. *Renew. Sustain. Energy Rev.* **2015**, *52*, 793–801. [[CrossRef](#)]
32. Menbari, A.; Alemrajabi, A.A.; Rezaei, A. Heat transfer analysis and the effect of cuo/water nanofluid on direct absorption concentrating solar collector. *Appl. Therm. Eng.* **2016**, *104*, 176–183. [[CrossRef](#)]
33. Hatami, M.; Mosayebidorcheh, S.; Jing, D. Thermal performance evaluation of alumina-water nanofluid in an inclined direct absorption solar collector (idasc) using numerical method. *J. Mol. Liq.* **2017**, *231*, 632–639. [[CrossRef](#)]
34. Colangelo, G.; Favale, E.; Miglietta, P.; de Risi, A.; Milanese, M.; Laforgia, D. Experimental test of an innovative high concentration nanofluid solar collector. *Appl. Energy* **2015**, *154*, 874–881. [[CrossRef](#)]
35. Li, Q.; Zheng, C.; Shirazi, A.; Mousa, O.B.; Moscia, F.; Scott, J.A.; Taylor, R.A. Design and analysis of a medium-temperature, concentrated solar thermal collector for air-conditioning applications. *Appl. Energy* **2017**, *190*, 1159–1173. [[CrossRef](#)]
36. Mahesh, A. Solar collectors and adsorption materials aspects of cooling system. *Renew. Sustain. Energy Rev.* **2017**, *73*, 1300–1312. [[CrossRef](#)]
37. Sardarabadi, M.; Passandideh-Fard, M.; Heris, S.Z. Experimental investigation of the effects of silica/water nanofluid on pv/t (photovoltaic thermal units). *Energy* **2014**, *66*, 264–272. [[CrossRef](#)]
38. Sarsam, W.S.; Amiri, A.; Kazi, S.; Badarudin, A. Stability and thermophysical properties of non-covalently functionalized graphene nanoplatelets nanofluids. *Energy Convers. Manag.* **2016**, *116*, 101–111. [[CrossRef](#)]
39. Moldoveanu, G.M.; Huminic, G.; Minea, A.A.; Huminic, A. Experimental study on thermal conductivity of stabilized Al₂O₃ and SiO₂ nanofluids and their hybrid. *Int. J. Heat Mass Transf.* **2018**, *127*, 450–457. [[CrossRef](#)]
40. Khodadadi, H.; Toghraie, D.; Karimipour, A. Effects of nanoparticles to present a statistical model for the viscosity of mgo-water nanofluid. *Powder Technol.* **2019**, *342*, 166–180. [[CrossRef](#)]
41. Akilu, S.; Baheta, A.T.; Kadirgama, K.; Padmanabhan, E.; Sharma, K. Viscosity, electrical and thermal conductivities of ethylene and propylene glycol-based β-sic nanofluids. *J. Mol. Liq.* **2019**, *284*, 780–792. [[CrossRef](#)]
42. Cai, Y.; Nan, Y.; Guo, Z. Enhanced absorption of solar energy in a daylighting louver with Ni-water nanofluid. *Int. J. Heat Mass Transf.* **2020**, *158*, 119921. [[CrossRef](#)]
43. Esfe, M.H.; Raki, H.R.; Emami, M.R.S.; Afrand, M. Viscosity and rheological properties of antifreeze based nanofluid containing hybrid nano-powders of mwcnts and TiO₂ under different temperature conditions. *Powder Technol.* **2019**, *342*, 808–816. [[CrossRef](#)]
44. Li, F.; Li, L.; Zhong, G.; Zhai, Y.; Li, Z. Effects of ultrasonic time, size of aggregates and temperature on the stability and viscosity of Cu-ethylene glycol (eg) nanofluids. *Int. J. Heat Mass Transf.* **2019**, *129*, 278–286. [[CrossRef](#)]
45. Esfe, M.H.; Bahiraei, M.; Mahian, O. Experimental study for developing an accurate model to predict viscosity of cuo-ethylene glycol nanofluid using genetic algorithm based neural network. *Powder Technol.* **2018**, *338*, 383–390. [[CrossRef](#)]
46. Doganay, S.; Turgut, A.; Cetin, L. Magnetic field dependent thermal conductivity measurements of magnetic nanofluids by 3ω method. *J. Magn. Magn. Mater.* **2019**, *474*, 199–206. [[CrossRef](#)]
47. Sidik, N.A.C.; Yazid, M.N.A.W.M.; Samion, S. A review on the use of carbon nanotubes nanofluid for energy harvesting system. *Int. J. Heat Mass Transf.* **2017**, *111*, 782–794. [[CrossRef](#)]

48. Aparna, Z.; Michael, M.; Pabi, S.; Ghosh, S. Thermal conductivity of aqueous Al₂O₃/Ag hybrid nanofluid at different temperatures and volume concentrations: An experimental investigation and development of new correlation function. *Powder Technol.* **2019**, *343*, 714–722. [[CrossRef](#)]
49. Xu, G.; Fu, J.; Dong, B.; Quan, Y.; Song, G. A novel method to measure thermal conductivity of nanofluids. *Int. J. Heat Mass Transf.* **2019**, *130*, 978–988. [[CrossRef](#)]
50. Keyvani, M.; Afrand, M.; Toghraie, D.; Reiszadeh, M. An experimental study on the thermal conductivity of cerium oxide/ethylene glycol nanofluid: Developing a new correlation. *J. Mol. Liq.* **2018**, *266*, 211–217. [[CrossRef](#)]
51. Bahiraei, M.; Rahmani, R.; Yaghoobi, A.; Khodabandeh, E.; Mashayekhi, R.; Amani, M. Recent research contributions concerning use of nanofluids in heat exchangers: A critical review. *Appl. Therm. Eng.* **2018**, *133*, 137–159. [[CrossRef](#)]
52. Nazarzade, S.; Ghorbani, H.R.; Jafarpourgolroudbary, H. Synthesis, preparation and the experimental study of silver/water nanofluid to optimize convective heat transfer in a shell and tube heat exchanger. *Inorg. Nano-Metal Chem.* **2019**, *49*, 173–176. [[CrossRef](#)]
53. Ullah, R.; Ishtiaq, T.M.; Mamun, A.H. Heat transfer enhancement in shell and tube heat exchanger by using Al₂O₃/water and TiO₂/water nanofluid. *AIP Conf. Proc.* **2019**, *2121*, 070018. [[CrossRef](#)]
54. Said, Z.; Rahman, S.; Assad, M.E.H.; Alami, A.H. Heat transfer enhancement and life cycle analysis of a shell-and-tube heat exchanger using stable CuO/water nanofluid. *Sustain. Energy Technol. Assess.* **2019**, *31*, 306–317. [[CrossRef](#)]
55. Somasekhar, K.; Rao, K.M.; Sankararao, V.; Mohammed, R.; Veerendra, M.; Venkateswararao, T. A CFD Investigation of Heat Transfer Enhancement of Shell and Tube Heat Exchanger Using Al₂O₃-Water Nanofluid. *Mater. Today Proc.* **2018**, *5*, 1057–1062. [[CrossRef](#)]
56. Esfahani, M.R.; Languri, E.M. Exergy analysis of a shell-and-tube heat exchanger using graphene oxide nanofluids. *Exp. Therm. Fluid Sci.* **2017**, *83*, 100–106. [[CrossRef](#)]
57. Bahmani, M.H.; Sheikhzadeh, G.; Zarringhalam, M.; Akbari, O.A.; Alrashed, A.A.; Shabani, G.A.S.; Goodarzi, M. Investigation of turbulent heat transfer and nanofluid flow in a double pipe heat exchanger. *Adv. Powder Technol.* **2018**, *29*, 273–282. [[CrossRef](#)]
58. Bahiraei, M.; Naghibzadeh, S.M.; Jamshidmofid, M. Efficacy of an eco-friendly nanofluid in a miniature heat exchanger regarding to arrangement of silver nanoparticles. *Energy Convers. Manag.* **2017**, *144*, 224–234. [[CrossRef](#)]
59. Sarafraz, M.; Hormozi, F. Intensification of forced convection heat transfer using biological nanofluid in a double-pipe heat exchanger. *Exp. Therm. Fluid Sci.* **2015**, *66*, 279–289. [[CrossRef](#)]
60. Sözen, A.; Variyenli, H.I.; Özdemir, M.B.; Gürü, M.; Aytac, I. Heat transfer enhancement using alumina and fly ash nanofluids in parallel and cross-flow concentric tube heat exchangers. *J. Energy Inst.* **2016**, *89*, 414–424. [[CrossRef](#)]
61. Saeedan, M.; Nazar, A.R.S.; Abbasi, Y.; Karimi, R. Cfd investigation and neutral network modeling of heat transfer and pressure drop of nanofluids in double pipe helically baffled heat exchanger with a 3-d fined tube. *Appl. Therm. Eng.* **2016**, *100*, 721–729. [[CrossRef](#)]
62. Shakiba, A.; Vahedi, K. Numerical analysis of magnetic field effects on hydro-thermal behaviour of a magnetic nanofluid in a double pipe heat exchanger. *J. Magn. Magn. Mater.* **2016**, *402*, 131–142. [[CrossRef](#)]
63. Kumar, N.R.; Bhramara, P.; Addis, B.M.; Sundar, L.S.; Singh, M.K.; Sousa, A.C. Heat transfer, friction factor and effectiveness analysis of Fe₃O₄/water nanofluid flow in a double pipe heat exchanger with return bend. *Int. Commun. Heat Mass Transf.* **2017**, *81*, 155–163. [[CrossRef](#)]
64. Ali, A.Y.M.; El-Shazly, A.H.; El-Kady, M.; Fathi, H.I.; El-Marghany, M.R. Effect of using MgO-Oil nanofluid on the performance of a counter-flow double pipe heat exchanger. *Key Eng. Mater.* **2019**, *801*, 193–198. [[CrossRef](#)]
65. Sun, B.; Peng, C.; Zuo, R.; Yang, D.; Li, H. Investigation on the flow and convective heat transfer characteristics of nanofluids in the plate heat exchanger. *Exp. Therm. Fluid Sci.* **2016**, *76*, 75–86. [[CrossRef](#)]
66. Elias, M.M.; Saidur, R.; Ben-Mansour, R.; Hepbasli, A.; Rahim, N.A.; Jesbains, K. Heat transfer and pressure drop characteristics of a plate heat exchanger using water based Al₂O₃ nanofluid for 30° and 60° chevron angles. *Heat Mass Transf.* **2018**, *54*, 2907–2916. [[CrossRef](#)]
67. Attalla, M.; Maghrabie, H.M. An experimental study on heat transfer and fluid flow of rough plate heat exchanger using Al₂O₃/water nanofluid. *Exp. Heat Transf.* **2020**, *33*, 261–281. [[CrossRef](#)]
68. Sarafraz, M.; Nikkhah, V.; Madani, S.; Jafarian, M.; Hormozi, F. Low-frequency vibration for fouling mitigation and intensification of thermal performance of a plate heat exchanger working with CuO/water nanofluid. *Appl. Therm. Eng.* **2017**, *121*, 388–399. [[CrossRef](#)]
69. Taghizadeh-Tabari, Z.; Heris, S.Z.; Moradi, M.; Kahani, M. The study on application of TiO₂/water nanofluid in plate heat exchanger of milk pasteurization industries. *Renew. Sustain. Energy Rev.* **2016**, *58*, 1318–1326. [[CrossRef](#)]
70. Pourhoseini, S.; Naghizadeh, N. An experimental study on optimum concentration of silver-water microfluid for enhancing heat transfer performance of a plate heat exchanger. *J. Taiwan Inst. Chem. Eng.* **2017**, *75*, 220–227. [[CrossRef](#)]
71. Behrangzade, A.; Heyhat, M.M. The effect of using nano-silver dispersed water based nanofluid as a passive method for energy efficiency enhancement in a plate heat exchanger. *Appl. Therm. Eng.* **2016**, *102*, 311–317. [[CrossRef](#)]
72. Pourhoseini, S.; Naghizadeh, N.; Hoseinzadeh, H. Effect of silver-water nanofluid on heat transfer performance of a plate heat exchanger: An experimental and theoretical study. *Powder Technol.* **2018**, *332*, 279–286. [[CrossRef](#)]
73. Anoop, K.; Sadr, R.; Yu, J.; Kang, S.; Jeon, S.; Banerjee, D. Experimental study of forced convective heat transfer of nanofluids in a microchannel. *Int. Commun. Heat Mass Transf.* **2012**, *39*, 1325–1330. [[CrossRef](#)]

74. Anoop, K.; Cox, J.; Sadr, R. Thermal evaluation of nanofluids in heat exchangers. *Int. Commun. Heat Mass Transf.* **2013**, *49*, 5–9. [CrossRef]
75. Sarafraz, M.; Hormozi, F. Heat transfer, pressure drop and fouling studies of multi-walled carbon nanotube nano-fluids inside a plate heat exchanger. *Exp. Therm. Fluid Sci.* **2016**, *72*, 1–11. [CrossRef]
76. Goodarzi, M.; Amiri, A.; Goodarzi, M.S.; Safaei, M.R.; Karimipour, A.; Languri, E.M.; Dahari, M. Investigation of heat transfer and pressure drop of a counter flow corrugated plate heat exchanger using MWCNT based nanofluids. *Int. Commun. Heat Mass Transf.* **2015**, *66*, 172–179. [CrossRef]
77. Kumar, V.; Tiwari, A.K.; Ghosh, S.K. Effect of chevron angle on heat transfer performance in plate heat exchanger using ZnO/water nanofluid. *Energy Convers. Manag.* **2016**, *118*, 142–154. [CrossRef]
78. Ramezanizadeh, M.; Ahmadi, M.H.; Nazari, M.A.; Sadeghzadeh, M.; Chen, L. A review on the utilized machine learning approaches for modeling the dynamic viscosity of nanofluids. *Renew. Sustain. Energy Rev.* **2019**, *114*, 109345. [CrossRef]
79. Elsheikh, A.H.; Sharshir, S.W.; Abd Elaziz, M.; Kabeel, A.E.; Guilan, W.; Haiou, Z. Modeling of solar energy systems using artificial neural network: A comprehensive review. *Sol. Energy* **2019**, *180*, 622–639. [CrossRef]
80. Yan, S.; Wang, F.; Shi, Z.; Tian, R. Heat transfer property of SiO₂/water nanofluid flow inside solar collector vacuum tubes. *Appl. Therm. Eng.* **2017**, *118*, 385–391. [CrossRef]
81. Moldoveanu, G.M.; Minea, A.A.; Humnic, G.; Humnic, A. Al₂O₃/TiO₂ hybrid nanofluids thermal conductivity. *J. Therm. Anal. Calorim.* **2019**, *137*, 583–592. [CrossRef]
82. Esfe, M.H.; Saedodin, S.; Yan, W.-M.; Afrand, M.; Sina, N. Study on thermal conductivity of water-based nanofluids with hybrid suspensions of CNTs/Al₂O₃ nanoparticles. *J. Therm. Anal. Calorim.* **2016**, *124*, 455–460. [CrossRef]
83. Moldoveanu, G.M.; Ibanescu, C.; Danu, M.; Minea, A.A. Viscosity estimation of Al₂O₃, SiO₂ nanofluids and their hybrid: An experimental study. *J. Mol. Liq.* **2018**, *253*, 188–196. [CrossRef]
84. Maxwell, J.C. *A Treatise on Electricity and Magnetism: Pt. III. Magnetism. pt. IV. Electromagnetism*; Clarendon Press: Oxford, UK, 1881; Volume 2, Available online: <https://www.aproged.pt/biblioteca/MaxwellIII.pdf> (accessed on 31 December 2023).
85. Hamilton, R.L.; Crosser, O.K. Thermal conductivity of heterogeneous two component systems. *Ind. Eng. Chem. Fundam.* **1962**, *1*, 187–191. [CrossRef]
86. Koo, J.; Kleinstreuer, C. A new thermal conductivity model for nanofluids. *J. Nanoparticle Res.* **2004**, *6*, 577–588. [CrossRef]
87. Sundar, L.S.; Mesfin, S.; Ramana, E.V.; Said, Z.; Sousa, A.C. Experimental investigation of thermo-physical properties, heat transfer, pumping power, entropy generation, and exergy efficiency of nanodiamond + Fe₃O₄/60:40% water-ethylene glycol hybrid nanofluid flow in a tube. *Therm. Sci. Eng. Prog.* **2021**, *21*, 100799. [CrossRef]
88. Esfahani, J.; Safaei, M.R.; Goharimanesh, M.; de Oliveira, L.R.; Goodarzi, M.; Shamshirband, S.; Filho, E.P.B. Comparison of experimental data, modelling and non-linear regression on transport properties of mineral oil based nanofluids. *Powder Technol.* **2017**, *317*, 458–470. [CrossRef]
89. Rostamian, S.H.; Biglari, M.; Saedodin, S.; Esfe, M.H. An inspection of thermal conductivity of CuO-SWCNTS hybrid nanofluid versus temperature and concentration using experimental data, ANN modelling and new correlation. *J. Mol. Liq.* **2017**, *231*, 364–369. [CrossRef]
90. Ahmadi, M.H.; Nazari, M.A.; Ghasempour, R.; Madah, H.; Shafii, M.B.; Ahmadi, M.A. Thermal conductivity ratio prediction of Al₂O₃/water nanofluid by applying connectionist methods. *Colloids Surf. A Physicochem. Eng. Asp.* **2018**, *541*, 154–164. [CrossRef]
91. Alade, I.O.; Oyehan, T.A.; Popoola, I.K.; Olatunji, S.O.; Bagudu, A. Modeling thermal conductivity enhancement of metal and metallic oxide nanofluids using support vector regression. *Adv. Powder Technol.* **2018**, *29*, 157–167. [CrossRef]
92. Esfe, M.H.; Esfandeh, S.; Afrand, M.; Rejvani, M.; Rostamian, S.H. Experimental evaluation, new correlation proposing and ANN modeling of thermal properties of EG based hybrid nanofluid containing zno-dwcnt nanoparticles for internal combustion engines applications. *Appl. Therm. Eng.* **2018**, *133*, 452–463. [CrossRef]
93. Ahmadi, M.H.; Nazari, M.A.; Mahian, O.; Ghasempour, R. A proposed model to predict thermal conductivity ratio of Al₂O₃/EG nanofluid by applying least squares support vector machine (LSSVM) and genetic algorithm as a connectionist approach. *J. Therm. Anal. Calorim.* **2019**, *135*, 271–281. [CrossRef]
94. Akhgar, A.; Toghraie, D.; Sina, N.; Afrand, M. Developing dissimilar artificial neural networks (ANNs) to prediction the thermal conductivity of MWCNT-TiO₂/water-ethylene glycol hybrid nanofluid. *Powder Technol.* **2019**, *355*, 602–610. [CrossRef]
95. Shahsavari, A.; Khanmohammadi, S.; Karimipour, A.; Goodarzi, M. A novel comprehensive experimental study concerned synthesizes and prepare liquid paraffin-Fe₃O₄ mixture to develop models for both thermal conductivity & viscosity: A new approach of GMDH type of neural network. *Int. J. Heat Mass Transf.* **2019**, *131*, 432–441. [CrossRef]
96. Rostami, S.; Kalbasi, R.; Sina, N.; Goldanlou, A.S. Forecasting the thermal conductivity of a nanofluid using artificial neural networks. *J. Therm. Anal. Calorim.* **2021**, *145*, 2095–2104. [CrossRef]
97. Sharma, P.; Ramesh, K.; Parameshwaran, R.; Deshmukh, S.S. Thermal conductivity prediction of titania-water nanofluid: A case study using different machine learning algorithms. *Case Stud. Therm. Eng.* **2022**, *30*, 101658. [CrossRef]
98. Sahin, F.; Genc, O.; Gökçek, M.; Çolak, A.B. An experimental and new study on thermal conductivity and zeta potential of Fe₃O₄/water nanofluid: Machine learning modeling and proposing a new correlation. *Powder Technol.* **2023**, *420*, 118388. [CrossRef]
99. Martyr, A.; Plint, M. *Engine Testing: The Design, Building, Modification and Use of Powertrain Test Facilities*; Elsevier: Amsterdam, The Netherlands, 2012. [CrossRef]

100. Phuoc, T.X.; Massoudi, M. Experimental observations of the effects of shear rates and particle concentration on the viscosity of Fe₂O₃-deionized water nanofluids. *Int. J. Therm. Sci.* **2009**, *48*, 1294–1301. [[CrossRef](#)]
101. Einstein, A. A new determination of molecular dimensions. *Ann. Phys.* **1906**, *19*, 289–306. [[CrossRef](#)]
102. Andrade, E.N.D.C. The viscosity of liquids. *Nature* **1930**, *125*, 309–310. [[CrossRef](#)]
103. Batchelor, G.K. The effect of brownian motion on the bulk stress in a suspension of spherical particles. *J. Fluid Mech.* **1977**, *83*, 97–117. [[CrossRef](#)]
104. Bicerano, J.; Douglas, J.F.; Brune, D.A. Model for the viscosity of particle dispersions. *J. Macromol. Sci. Part C Polym. Rev.* **1999**, *39*, 561–642. [[CrossRef](#)]
105. Vajjha, R.S. Measurements of Thermophysical Properties of Nanofluids and Computation of Heat Transfer Characteristics. Ph.D. Thesis, University of Alaska Fairbanks, Fairbanks, AK, USA, 2008.
106. Alrashed, A.A.; Gharibdousti, M.S.; Goodarzi, M.; de Oliveira, L.R.; Safaei, M.R.; Filho, E.P.B. Effects on thermophysical properties of carbon based nanofluids: Experimental data, modelling using regression, ANFIS and ANN. *Int. J. Heat Mass Transf.* **2018**, *125*, 920–932. [[CrossRef](#)]
107. Hemmat Esfe, M.; Rostamian, H.; Esfandeh, S.; Afrand, M. Modeling and prediction of rheological behavior of Al₂O₃-mwcnt/5w50 hybrid nano-lubricant by artificial neural network using experimental data. *Phys. A Stat. Mech. Its Appl.* **2018**, *510*, 625–634. [[CrossRef](#)]
108. Demirpolat, A.B.; Das, M. Prediction of viscosity values of nanofluids at different pH values by alternating decision tree and multilayer perceptron methods. *Appl. Sci.* **2019**, *9*, 1288. [[CrossRef](#)]
109. Ghaffarkhah, A.; Bazzi, A.; Dijvejin, Z.A.; Talebkeikhah, M.; Moraveji, M.K.; Agin, F. Experimental and numerical analysis of rheological characterization of hybrid nano-lubricants containing COOH-Functionalized MWCNTs and oxide nanoparticles. *Int. Commun. Heat Mass Transf.* **2019**, *101*, 103–115. [[CrossRef](#)]
110. Toghraie, D.; Sina, N.; Jolfaei, N.A.; Hajian, M.; Afrand, M. Designing an artificial neural network (ANN) to predict the viscosity of silver/ethylene glycol nanofluid at different temperatures and volume fraction of nanoparticles. *Phys. A Stat. Mech. Its Appl.* **2019**, *534*, 122142. [[CrossRef](#)]
111. Ahmadi, M.H.; Mohseni-Gharyehsafa, B.; Ghazvini, M.; Goodarzi, M.; Jilte, R.D.; Kumar, R. Comparing various machine learning approaches in modeling the dynamic viscosity of CuO/water nanofluid. *J. Therm. Anal. Calorim.* **2020**, *139*, 2585–2599. [[CrossRef](#)]
112. Gholizadeh, M.; Jamei, M.; Ahmadianfar, I.; Pourrajab, R. Prediction of nanofluids viscosity using random forest (RF) approach. *Chemom. Intell. Lab. Syst.* **2020**, *201*, 104010. [[CrossRef](#)]
113. Kanti, P.; Sharma, K.V.; Yashawantha, K.M.; Dmk, S. Experimental determination for viscosity of fly ash nanofluid and fly ash-Cu hybrid nanofluid: Prediction and optimization using artificial intelligent techniques. *Energy Sources Part A Recover. Util. Environ. Eff.* **2021**, 1–20. [[CrossRef](#)]
114. Dai, X.; Andani, H.T.; Alizadeh, A.; Abed, A.M.; Smaisim, G.F.; Hadrawi, S.K.; Karimi, M.; Shamsborhan, M.; Toghraie, D. Using gaussian process regression (GPR) models with the matern covariance function to predict the dynamic viscosity and torque of SiO₂/ethylene glycol nanofluid: A machine learning approach. *Eng. Appl. Artif. Intell.* **2023**, *122*, 106107. [[CrossRef](#)]
115. Freire, E. *Differential Scanning Calorimetry*; Humana Press: Totowa, NJ, USA, 1995; pp. 191–218. [[CrossRef](#)]
116. Higano, M.; Miyagawa, A.; Saigou, K.; Masuda, H.; Miyashita, H. Measuring the specific heat capacity of magnetic fluids using a differential scanning calorimeter. *Int. J. Thermophys.* **1999**, *20*, 207–215. [[CrossRef](#)]
117. Tiznobaik, H.; Shin, D. Enhanced specific heat capacity of high-temperature molten salt-based nanofluids. *Int. J. Heat Mass Transf.* **2013**, *57*, 542–548. [[CrossRef](#)]
118. Shahrul, I.; Mahbulul, I.; Khaleduzzaman, S.; Saidur, R.; Sabri, M. A comparative review on the specific heat of nanofluids for energy perspective. *Renew. Sustain. Energy Rev.* **2014**, *38*, 88–98. [[CrossRef](#)]
119. Pak, B.C.; Cho, Y.I. Hydrodynamic and heat transfer study of dispersed fluids with submicron metallic oxide particles. *Exp. Heat Transf.* **1998**, *11*, 151–170. [[CrossRef](#)]
120. Xuan, Y.; Roetzel, W. Conceptions for heat transfer correlation of nanofluids. *Int. J. Heat Mass Transf.* **2000**, *43*, 3701–3707. [[CrossRef](#)]
121. Sundar, L.S.; Singh, M.K.; Sousa, A.C. Turbulent heat transfer and friction factor of nanodiamond-nickel hybrid nanofluids flow in a tube: An experimental study. *Int. J. Heat Mass Transf.* **2018**, *117*, 223–234. [[CrossRef](#)]
122. Alade, I.O.; Rahman, M.A.A.; Saleh, T.A. Predicting the specific heat capacity of alumina/ethylene glycol nanofluids using support vector regression model optimized with bayesian algorithm. *Sol. Energy* **2019**, *183*, 74–82. [[CrossRef](#)]
123. Hassan, M.A.; Banerjee, D. A soft computing approach for estimating the specific heat capacity of molten salt-based nanofluids. *J. Mol. Liq.* **2019**, *281*, 365–375. [[CrossRef](#)]
124. Alade, I.O.; Rahman, M.A.A.; Abbas, Z.; Yaakob, Y.; Saleh, T.A. Application of support vector regression and artificial neural network for prediction of specific heat capacity of aqueous nanofluids of copper oxide. *Sol. Energy* **2020**, *197*, 485–490. [[CrossRef](#)]
125. Daneshfar, R.; Bemani, A.; Hadipoor, M.; Sharifpur, M.; Ali, H.M.; Mahariq, I.; Abdeljawad, T. Estimating the heat capacity of non-newtonian ionanofluid systems using ann, anfis, and sgb tree algorithms. *Appl. Sci.* **2020**, *10*, 6432. [[CrossRef](#)]
126. Adun, H.; Kavaz, D.; Wole-Osho, I.; Dagbasi, M. Synthesis of Fe₃O₄-Al₂O₃-ZnO/water ternary hybrid nanofluid: Investigating the effects of temperature, volume concentration and mixture ratio on specific heat capacity, and development of hybrid machine learning for prediction. *J. Energy Storage* **2021**, *41*, 102947. [[CrossRef](#)]

127. Jamei, M.; Karbasi, M.; Olumegbon, I.A.; Mosharaf-Dehkordi, M.; Ahmadianfar, I.; Asadi, A. Specific heat capacity of molten salt-based nanofluids in solar thermal applications: A paradigm of two modern ensemble machine learning methods. *J. Mol. Liq.* **2021**, *335*, 116434. [CrossRef]
128. Zhang, Y.; Xu, X. Machine learning specific heat capacities of nanofluids containing CuO and Al₂O₃. *AIChE J.* **2021**, *67*, e17289. [CrossRef]
129. Said, Z.; Sharma, P.; Elavarasan, R.M.; Tiwari, A.K.; Rathod, M.K. Exploring the specific heat capacity of water-based hybrid nanofluids for solar energy applications: A comparative evaluation of modern ensemble machine learning techniques. *J. Energy Storage* **2022**, *54*, 105230. [CrossRef]
130. McCulloch, W.S.; Pitts, W.H. A logical calculus of the ideas immanent in nervous activity. *Bull. Math. Biophys.* **1943**, *5*, 115–133. [CrossRef]
131. Rumelhart, D.E.; Hinton, G.E.; Williams, R.J. Learning representations by back-propagating errors. *Nature* **1986**, *323*, 533–536. [CrossRef]
132. LeCun, Y.; Bengio, Y.; Hinton, G. Deep learning. *Nature* **2015**, *521*, 436–444. [CrossRef] [PubMed]
133. Ruder, S. An overview of gradient descent optimization algorithms. *arXiv* **2016**, arXiv:1609.04747. [CrossRef]
134. Krizhevsky, A.; Sutskever, I.; Hinton, G.E. Imagenet classification with deep convolutional neural networks. *Adv. Neural Inf. Process. Syst.* **2012**, *25*, 84–90. Available online: https://proceedings.neurips.cc/paper_files/paper/2012/file/c399862d3b9d6b76c8436e924a68c45b-Paper.pdf (accessed on 31 December 2023). [CrossRef]
135. Jordan, M.I.; Mitchell, T.M. Machine learning: Trends, perspectives, and prospects. *Science* **2015**, *349*, 255–260. [CrossRef]
136. Chen, S.; Cowan, C.; Grant, P. Orthogonal least squares learning algorithm for radial basis function networks. *IEEE Trans. Neural Netw.* **1991**, *2*, 302–309. [CrossRef]
137. Broomhead, D.; Lowe, D. Multivariable functional interpolation and adaptive networks. *Complex Syst.* **1988**, *2*, 321–355. Available online: <https://sci2s.ugr.es/keel/pdf/algorithm/articulo/1988-Broomhead-CS.pdf> (accessed on 31 December 2023).
138. Ivakhnenko, A.G. The group method of data handling, a rival of the method of stochastic approximation. *Sov. Autom. Control* **1968**, *13*, 43–55.
139. Vapnik, V.N. A note on one class of perceptrons. *Automat. Rem. Control.* **1964**, *25*, 821–837. Available online: <https://classes.engr.oregonstate.edu/eecs/fall2023/ai534-400/extra/vapnik-1964.pdf> (accessed on 31 December 2023).
140. Cortes, C.; Vapnik, V. Support-vector networks. *Mach. Learn.* **1995**, *20*, 273–297. [CrossRef]
141. Boser, B.E.; Guyon, I.M.; Vapnik, V.N. A training algorithm for optimal margin classifiers. In Proceedings of the Fifth Annual Workshop on Computational Learning Theory, Pittsburgh, PA, USA, 27–29 July 1992; pp. 144–152. [CrossRef]
142. Cohn, T.; Preotiuc-Pietro, D.; Lawrence, N. Gaussian Processes for Natural Language Processing. In Proceedings of the 52nd Annual Meeting of the Association for Computational Linguistics: Tutorials, Association for Computational Linguistics, Baltimore, MD, USA, 22 June 2014; pp. 1–3. [CrossRef]
143. Wistuba, M.; Rawat, A. Scalable multi-class bayesian support vector machines for structured and unstructured data. *arXiv* **2018**, arXiv:1806.02659. [CrossRef]
144. Law, T.; Shawe-Taylor, J. Practical bayesian support vector regression for financial time series prediction and market condition change detection. *Quant. Financ.* **2017**, *17*, 1403–1416. [CrossRef]
145. Xu, H.; Song, S.; Li, J.; Guo, T. Hybrid model for daily runoff interval predictions based on bayesian inference. *Hydrol. Sci. J.* **2023**, *68*, 62–75. [CrossRef]
146. Nurwaha, D. Comparison of kernel functions of support vector machines: A case study for the solar cell output power prediction. *Int. J. Energy Appl. Technol.* **2020**, *7*, 1–6. [CrossRef]
147. Wirasati, I.; Rustam, Z.; Aurelia, J.E.; Hartini, S.; Saragih, G.S. Comparison some of kernel functions with support vector machines classifier for thalassemia dataset. *IAES Int. J. Artif. Intell.* **2021**, *10*, 430. [CrossRef]
148. Thorstan, J. Text categorization with support vector machines: Learning with many relevant features. In Proceedings of the European Conference on Machine Learning, Chemnitz, Germany, 21–23 April 1998; Springer: Berlin/Heidelberg, Germany, 1998; pp. 137–142. [CrossRef]
149. Burges, C.J.C. A tutorial on support vector machines for pattern recognition. *Data Min. Knowl. Discov.* **1998**, *2*, 121–167. [CrossRef]
150. Scholkopf, B.; Smola, A.J.; Williamson, R.C.; Bartlett, P.L. New Support Vector Algorithms. *Neural Comput.* **2000**, *12*, 1207–1245. [CrossRef]
151. Breiman, L. *Classification and Regression Trees*; Routledge: Boca Raton, FL, USA, 1984. [CrossRef]
152. Quinlan, J.R. Induction of decision trees. *Mach. Learn.* **1986**, *1*, 81–106. [CrossRef]
153. Halalshah, N.; Alshboul, O.; Shehadeh, A.; Al Mamlook, R.E.; Al-Othman, A.; Tawalbeh, M.; Almuflih, A.S.; Papelis, C. Breakthrough curves prediction of selenite adsorption on chemically modified zeolite using boosted decision tree algorithms for water treatment applications. *Water* **2022**, *14*, 2519. [CrossRef]
154. Freund, Y.; Mason, L. The alternating decision tree learning algorithm. In Proceedings of the 16th International Conference on Machine Learning, San Francisco, CA, USA, 27–30 June 1999; Available online: <https://csweb.ucsd.edu/~yfreund/papers/atrees.pdf> (accessed on 4 March 2024).
155. Nepomuceno-Chamorro, I.A.; Aguilar-Ruiz, J.S.; Riquelme, J.C. Inferring gene regression networks with model trees. *BMC Bioinform.* **2010**, *11*, 517. [CrossRef] [PubMed]

156. Prasetyaningrum, P.T.; Pratama, I.; Chandra, A.Y. Implementation of Machine Learning to Determine the Best Employees Using Random Forest Method. *Int. J. Comput. Netw. Secur. Inf. Syst.* **2021**, *2*, 53–59. [[CrossRef](#)]
157. Padmaja, B.; Prasa, V.; Sunitha, K. A novel random split point procedure using extremely randomized (extra) trees ensemble method for human activity recognition. *EAI Endorsed Trans. Pervasive Heal. Technol.* **2020**, *6*, e5. [[CrossRef](#)]
158. Chen, S.; Shen, B.; Wang, X.; Yoo, S.-J. A strong machine learning classifier and decision stumps based hybrid adaboost classification algorithm for cognitive radios. *Sensors* **2019**, *19*, 5077. [[CrossRef](#)]
159. Friedman, J.H. Greedy function approximation: A gradient boosting machine. *Ann. Stat.* **2001**, *29*, 1189–1232. [[CrossRef](#)]
160. Chen, T.; Guestrin, C. Xgboost: A scalable tree boosting system. In Proceedings of the 22nd Acm Sigkdd International Conference on Knowledge Discovery and Data Mining, San Francisco, CA, USA, 13–17 August 2016; pp. 785–794. [[CrossRef](#)]
161. Holland, J.H. Genetic Algorithms. *Sci. Am.* **1992**, *267*, 66–73. [[CrossRef](#)]
162. Goldberg, D.E. Genetic algorithms in search, Optimization. *Mach. Learn.* **1988**, *3*, 95–99. [[CrossRef](#)]
163. Mitchell, M. *An Introduction to Genetic Algorithms*; MIT Press: Cambridge, MA, USA, 1998. [[CrossRef](#)]
164. Gandomi, A.H.; Alavi, A.H. Multi-stage genetic programming: A new strategy to nonlinear system modeling. *Inf. Sci.* **2011**, *181*, 5227–5239. [[CrossRef](#)]
165. Garg, A.; Garg, A.; Tai, K.; Sreedeeep, S. An integrated srm-multi-gene genetic programming approach for prediction of factor of safety of 3-d soil nailed slopes. *Eng. Appl. Artif. Intell.* **2014**, *30*, 30–40. [[CrossRef](#)]
166. Jang, J.-S.R. Anfis: Adaptive-network-based fuzzy inference system. *IEEE Trans. Syst. Man Cybern.* **1993**, *23*, 665–685. [[CrossRef](#)]
167. Jang, J.-S.R.; Sun, C.-T.; Mizutani, E. Neuro-fuzzy and soft computing a computational approach to learning and machine intelligence [book review]. *IEEE Trans. Autom. Control* **1997**, *42*, 1482–1484. [[CrossRef](#)]
168. Amemiya, T. Non-Linear Regression Models. In *Handbook of Econometrics*; Elsevier: Amsterdam, The Netherlands, 1983; Volume 1, Chapter 6; pp. 333–389. [[CrossRef](#)]
169. Friedman, J.H. Multivariate Adaptive Regression Splines. *Ann. Stat.* **1991**, *19*, 1–67. [[CrossRef](#)]
170. Wilson, A.G.; Knowles, D.A.; Ghahramani, Z. Gaussian process regression networks. *arXiv* **2011**, arXiv:1110.4411. Available online: <https://arxiv.org/pdf/1110.4411.pdf> (accessed on 31 December 2023).
171. Yu, W.; Choi, S. The Role of Interfacial Layers in the Enhanced Thermal Conductivity of Nanofluids: A Renovated Maxwell Model. *J. Nanoparticle Res.* **2003**, *5*, 167–171. [[CrossRef](#)]
172. Jeffrey, D.J. Conduction through a random suspension of spheres. *Proc. R. Soc. Lond. A Math. Phys. Sci.* **1973**, *1602*, 355–367. [[CrossRef](#)]
173. Maïga, S.E.B.; Nguyen, C.T.; Galanis, N.; Roy, G. Heat transfer behaviours of nanofluids in a uniformly heated tube. *Superlattices Microstruct.* **2004**, *35*, 543–557. [[CrossRef](#)]
174. Esfe, M.H.; Afrand, M.; Yan, W.-M.; Yarmand, H.; Toghraie, D.; Dahari, M. Effects of temperature and concentration on rheological behavior of MWCNTs/SiO₂(20–80)-SAE40 hybrid nano-lubricant. *Int. Commun. Heat Mass Transf.* **2016**, *76*, 133–138. [[CrossRef](#)]
175. Wang, X.; Xu, X.; Choi, S.U.S. Thermal conductivity of nanoparticle—Fluid mixture. *J. Thermophys. Heat Transf.* **1999**, *13*, 474–480. [[CrossRef](#)]
176. Ma, T.; Guo, Z.; Lin, M.; Wang, Q. Recent trends on nanofluid heat transfer machine learning research applied to renewable energy. *Renew. Sustain. Energy Rev.* **2021**, *138*, 110494. [[CrossRef](#)]
177. Zhou, S.-Q.; Ni, R. Measurement of the specific heat capacity of water-based Al₂O₃ nanofluid. *Appl. Phys. Lett.* **2008**, *92*, 093123. [[CrossRef](#)]
178. Mendez, M.; Ianiro, A.; Noack, B.; Brunton, S. (Eds.) *Data-Driven Fluid Mechanics: Combining First Principles and Machine Learning*; Cambridge University Press: Cambridge, UK, 2023. [[CrossRef](#)]
179. Adun, H.; Wole-Osho, I.; Okonkwo, E.C.; Kavaz, D.; Dagbasi, M. A critical review of specific heat capacity of hybrid nanofluids for thermal energy applications. *J. Mol. Liq.* **2021**, *340*, 116890. [[CrossRef](#)]

Disclaimer/Publisher’s Note: The statements, opinions and data contained in all publications are solely those of the individual author(s) and contributor(s) and not of MDPI and/or the editor(s). MDPI and/or the editor(s) disclaim responsibility for any injury to people or property resulting from any ideas, methods, instructions or products referred to in the content.